PHOTODEGRADATION OF RHODAMINE B AND METHYL RED USING Cd-Al/AC and Cd-Sb/AC LAYERED DOUBLE HYDROXIDE CATALYSTS

BY

ABBA GARZALI FAGGE

SPS/15/MCH/00085

A DISSERTATION SUBMITTED TO THE DEPARTMENT OF PURE AND INDUSTRIAL CHEMISTRY, FACULTY OF PHYSICAL SCIENCES, BAYERO UNIVERSITY, KANO, IN PARTIAL FULLFILLMENT OF THE REQUIRMENTS FOR THE AWARD OF MASTER OF SCIENCE (M.Sc) DEGREE IN PHYSICAL CHEMISTRY

December, 2019.

DECLARATION

I hereby declared that this work is the product of my own research undertaken under the supervision of Dr. Abdulfatah S. Mohammed and has not been presented for the award of any other degree or certificate.

_____ _____

ABBA GARZALI FAGGE DATE

SPS/15/MCH/00085

CERTIFICATION

This is to certify that the research work for this dissertation and the subsequent write-up by Abba Garzali Fagge (SPS//15/MCH/00085) were carried out under supervision.

_____ _____

Dr. Abdulfatah S. Muhammad Date

(Supervisor)

APPROVAL PAGE

This dissertation has been examined and approved for the award of Master Degree in Physical Chemistry

_____	_____
Dr. Ahmad Galadima External Examiner	Date
_____	_____
Dr. Umar Ibrahim Gaya Internal Examiner	Date
_____	_____
Dr. Abdulfatah Shehu Muhammad Supervisor	Date
_____	_____
Dr. Ibrahim Tajo Suraj Head of Department	Date
_____	_____
Professor Sulaiman Yusuf Mudi Faculty of Physical Sciences SPS Representative	Date

DEDICATION

I dedicated this thesis to the almighty Allah (S.W.T) and noble prophet Muhammad (S.A.W.), then also to my parent late Alhaji Hamza and Hajiya Bilkisu, and my elder sister late Hajara Hamza, all brothers and sisters, friends well-wishers and all those who have contributed to my success in this program.

ACKNOWLEDGMENT

All praises be to almighty Allah (S.W.T.), the creator of all matter who in his infinite mercy provided me with good health, wealth, patience and wisdom to successfully accomplish this goal and may his ultimate mercy peace and blessing be upon his messenger Muhammad (S.A.W) and his followers. My gratitude also goes to my lecturer's especially my Supervisor Dr. Abdulfatah S Muhammad.

And finally my regards goes to all my collegues and friend at Pure and Industrial Chemistry Department who contributed in one way or the other during our studies, Ameen

TABLE OF CONTENTS

LIST OF FIGURES

LIST OF TABLES

ABSTRACT

The degradation of Rhodamine B and Methyl Red using (Cd-Al/AC) and (Cd-Sb/AC) layered double hydroxides under visible light was investigated. The layered double hydroxides were successfully prepared from cadmium fluoride (CdF_2), aluminum chloride ($AlCl_3$), rice husks activated carbon for Cd-Al/AC and ($SbCl_3$) for Cd-Sb/AC. The catalysts were characterized by X-ray Diffraction (XRD), Scanning Electron Microscopy (SEM) and Fourier Transform Infrared (FTIR) methods. The 2Ɵ peaks at 23.4^O and 35.5^O in the both Cd-Al/AC and Cd-Sb/AC XRD results confirmed the presence of LDH. The effect of initial dye concentration, pH and catalyst dosage on the photodegration of Rhodamine B and Methyl red were investigated. The highest percentages were achieved after 100 min, at 200 mg of either Cd-Al/AC or Cd-Sb/AC, at 3 ppm concentration (RB or MR), with percentage removal of 76.22%, 83.8%, 51.36% and 32.36% for RB using Cd-Al/AC, MR using Cd-Al/AC, RB using Cd-Sb/AC and MR using Cd-Sb/AC, respectively. For kinetics studies, the data obtained were modeled using pseudo first order and pseudo second order approaches. From the linear regression coefficient values, the data were found to be best fitted to pseudo second order kinetics. Overall Cd-Al/AC LDH showed better catalytic activity and this is probably due to its low band gap energy.

CHAPTER ONE

INTRODUCTION

1.1 Background of the Study

Water pollution occurs when unwanted materials enter into water, changes the quality of water and harmful to environment and human health (Alrumman *et al*., 2016). Water is an important natural resource used for drinking and other developmental purposes in our lives (Bibi *et al.,* 2016). Organic dyes used in textile manufacturing are considered to be an essential source of pollutants to the environment due to their non-biodegradability and high toxicity to aquatic creatures and carcinogenic effects on humans (Papic *et al.,* 2004). Therefore, organic dyes removal from waste waters has been one of the most important environmental issues and complete removal of organic dyes is essential because organic dyes will be perceptible even at low quantities (Papic *et al.,* 2004). In countries all over the world (developing and industrialized), the number of organic pollutants discharged into all kinds of open waters is on the rise (Shannon *et al.,* 2008).

A number of physical and chemical treatment processes including precipitation, adsorption, air stripping, flocculation, reverse osmosis and ultrafiltration are being employed for the removal of these toxic pollutants from water. Most of these methods suffer from various drawbacks (Jeanette *et al*., 2005). These methods are fairly effective in removing pollutants. However the main drawback of these techniques is formation of secondary waste product which cannot be treated again and dumped as such (Ferreira *et al*., 2001).

Photocatalysis is being considered as an efficient process for the mineralization of toxic organic dyes, due to the generation of hydroxyl radicals ($OH^{\bullet}$) which possess strong oxidizing potential (Aslan *et al.,* 2000). In all known AOPs, the heterogeneous photocatalytic process is the

most effective method because of its high availability, low toxicity, inexpensive and diverse nature that might attacked and mineralize a large number of contaminants (Khatee and Kasiri, 2010).

Several studies demonstrated that the group of hydrotalcites, which are layered double hydroxides (LDH) or anionic clays, are efficient materials to intercalated anionic compounds such as sulphate dyes and surfactants, halides, sulfates, nitrates, silicates, chlorides, and polymers (Barriga *et al*., 2002). Inorganic or organic anions can be introduced between hydroxide layer by ion exchange or Precipitation (Hirlekar et al., 2008). Anions are intercalated into the interlayers of Layered Double Hydroxide to maintain electroneutrality with water molecules (Ye et al., 2012).

1.2 CATALYSIS

Catalysis is the monitoring of the action of a catalyst on a reaction; and a catalyst is a substance that increases the rate of reaction without modifying the overall standard Gibbs energy change in the reaction (Permon *et al*., 2002). Catalysis has a very long term history and it is a natural process associated with the beginning of life itself. The favorability of a catalytic reaction compared to other processes is the fact that it takes place at low temperature, gives highly selected targets of our interest, less expensive, easily controllable; environmentally clean (Permon *et al.*, 2002).

Catalysis can be two types: homogeneous and heterogeneous. In homogeneous catalysis, reactants and catalyst are in the same phase. Acid-base and enzyme catalysis are examples of homogeneous catalysis. In heterogeneous catalysis reactant and catalyst are in the different phase. Catalysis by metals and semiconductors are examples of the heterogenous catalysis. Here reactions occur at the interface between the phases (Permon *et al*., 2002). The conversion of

wastes and raw materials into energy, reduction of greenhouse gases, conversion of monomers into polymer, production of material from cheap source etc are the key roles of the heterogenous catalysts. Thus, there is a tremendous pressure exerted on chemical manufacturing industry to develop new synthetic methods that are environment friendly and more acceptable by the catalysis field for the production of economic products. Photocatalysis plays a key role in this situation (Permon *et al*., 2002).

1.3 PHOTOCATALYSIS

Photocatalysis is a process where light and catalysts are concurrently used to support or speed up a chemical reaction. So, photocatalysis can be defined as "catalysis driven acceleration of a light-induced reaction" (Saravanan *et al*., 2017). A photocatalyst is a solid material; need to satisfy the following condition: (i) the molecule is adsorbed on the particle surface; (ii) the molecule undergoes chemical transformation while visiting several reaction surface sites by surface diffusion and (iii) the intermediate or product molecule is subsequently desorbed to the gas phase or to the condensed phase. The interactions between the reactant molecule and the photo catalyst's surface site must be such (not too strong or not too weak) that bond breaking and bond making can take place within the residence time of the intermediate(s), and that desorption/adsorption can occur. The catalyst may accelerate the photoreaction by interacting with the substrate(s) either in its ground state or in its excited state or with the primary product (of the catalyst), depending on the mechanism of the photoreaction (Somorjai 1989). Photocatalysis involves three processes: the excitation, bulk diffusion and surface transfer of photo induced charge carriers. These processes are influenced by the bulk structure, surface structure and electronic structure of the semiconductor photo catalysts.

1.3.1 History of Heteregeneous of Photocatalysis

Heterogeneous photocatalysis is a rapidly expanding technology for water and air treatment. It can be defined as the acceleration of photoreaction in the presence of a catalyst. The initial interest in the heterogeneous photocatalysis was started when Fujishima and Honda (1972) discovered that the photochemical splitting of water into hydrogen and oxygen can occur with TiO_2. From this date extensive work has been carried out to produce hydrogen from water by this novel oxidation reduction reaction using a variety of semiconductors (Fujishima and Honda, 1972). Interest has been focused on the use of semiconductor materials as photocatalysts for the removal of organic and inorganic species from aqueous or gas phase. This method has been suggested in environmental protection due to its ability to oxidise the organic and inorganic substrates (Fox and Dulay, 1993). In heterogeneous photocatalysis two or more phases are used in the photocatalytic reaction. A light source with semiconductor material is used to initiate the photoreaction. The catalysts can carry out substrate oxidations and reductions simultaneously. UV light of long wavelengths can be used, possibly even sunlight (Fox and Dulay, 1993).

Heterogeneous photocatalysis using semiconductors such as TiO_2 can be more interesting than conventional methods for removing organic species in the environment. Because the process gradually breaks down the contaminant molecule, no residue of the original material remains and therefore no sludge requiring disposal to landfill is produced (Ibhadon and Paul 2013). The catalyst itself is unchanged during the process and no consumable chemicals are required (Fox and Dulay, 1993). These results in considerable savings and a simpler operation of the equipment involved. Additionally, because the contaminant is attracted strongly to the surface of the catalyst, the process will continue to work at very low concentrations allowing sub part-per-million consents to be achieved. Taken together, these advantages mean that the process

results in considerable savings in the water production cost and keeping the environment clean (Ibhadon and Paul, 2013).

1.3.2 Principle of Photocatalysis

Photocatalysis over a semiconductor oxide such as TiO_2 is initiated by the absorption of a photon with energy equal to or greater than the band gap of the semiconductor (ca. 3.2 eV for anatase), producing electron-hole (*e*-/*h*+) pairs, as written in the equation (1) (Mills and Le 1997)

$$TiO_{2\text{----hv---------}} e^-_{cb}(TiO_2) + h^+_{vb}\,(TiO_2) \qquad (1)$$

where cb is conduction band and vb is the valence band. Consequently, following irradiation, the TiO_2 particle can act as either an electron donor or acceptor for molecules in the surrounding medium. The electron and hole can recombine, releasing the absorbed light energy as heat, with no chemical effect. Otherwise, the charges can move to "trap" sites at slightly lower energies. The charges can still recombine, or they participate in redox reactions with adsorbed species. A simplified mechanism for the photo-activation of a semiconductor catalyst. The valence band hole is strongly oxidizing, and the conduction band electron is strongly reducing. At the external surface, the excited electron and the hole can take part in redox reactions with adsorbed species such as water, hydroxide ion (OH^-), organic compounds, or oxygen. The charges can react directly with adsorbed pollutants, but reactions with water are far more likely since the water molecules are far more populous than contaminant molecules. Oxidation of water or OH^- by the hole produces the hydroxyl radical ($^{\bullet}OH$), an extremely powerful and indiscriminant oxidant. For a comparison, the oxidation potential of hydroxyl radical ($^{\bullet}OH$) is 2.8 V relative to the normal hydrogen electrode (NHE). Other substances used for water disinfection: ozone (2.07 V), H_2O_2 (1.78 V), HOCl (1.49 V) and chlorine (1.36 V) $^{\cdot}OH$ radicals rapidly attack pollutants at the

surface, and possibly in solution as well, and are usually the most important radicals formed in TiO_2 photocatalysis. An important reaction of the conduction band electron is reduction of adsorbed O_2 to $O_2^{\bullet -}$ (Mills and Le, 1997).

This reaction prevents the electron from recombining with the hole and results in an accumulation of oxygen radical species that can also participate in attacking contaminants (Rauf *et al.*, 2007).

1.3.3 Factors Influencing the Photocatalytic Degradation

The oxidation rates and efficiency of the photocatalytic systems are highly dependent on a number of operational parameters that govern the photodegradation of the organic molecule (Ng and Chen, 2012). Several studies have reported the significance of operational parameters.

a. Effect of Dye Concentration

The photocatalysis depends on the adsorption of dyes on the surface of photocatalyst. In the photocatalysis process, only the amount of dye adsorbed on the surface of photocatalyst contributes to the adsorption of the dye and not the one in the bulk of the solution. The adsorption of dye depends on the initial concentration of dye. The initial concentration of dye in a given photocatalytic reaction is an important factor which needs to be taken into account. Generally speaking the percentage degradation decreases with increasing amount of dye concentration, while keeping a fixed amount of catalyst, in order to know the effect of concentration (Reza *et al*., 2017) in order to study the effect of concentration.

b. Effect of Catalyst Amount

Degradation of dye is affected by the amount of the photocatalyst. The photodegradation of dye increases with increasing catalyst amount, which is the feature of heterogeneous

photocatalysis. The increase in catalyst amount actually increases the number of active sites on the photocatalyst surface thus causing an increase in the formation of number of $^{\bullet}OH$ radicals which can take part in actual discoloration of dye solution. Beyond a certain limit of catalyst amount, the solution becomes turbid and thus blocks UV radiation for the reaction to proceed and therefore percentage degradation starts decreasing (Reza *et al*., 2017).

c. Effect of pH

The Photodegradation of dyes is affected by the pH of the solution. The variation of solution pH changes the surface charge of catalyst particles and shifts the potentials of catalytic reactions. As a result, the adsorption of dye on the surface is altered thereby causing a change in the reaction rate. Under acidic or alkaline condition the surface of catalyst can be protonated or deprotonated, alkaline condition is the best for cationic dyes and acidic condition is the best for anionic dyes (Davis *et al*., 1994). The degradation rate of azo dyes increases with decrease in pH, at pH <6, a strong adsorption of the dye on the catalyst is observed as a result of the electrostatic attraction of the positively charged catalyst with the dye. At pH >6.8 as dye molecules are negatively charged in alkaline media, their adsorption is also expected to be affected by an increase in the density of catalyst on the semiconductor surface. Thus, due to Coulombic repulsion the dyes are scarcely adsorbed (Hameed and Akpan, 2009).

d. Effect of Surface Area

Surface morphology of catalyst is a crucial factor in its use as photocatalyst, as all the chemical events take place at the surface, its enlargement has been attempted, usually by using very fine particles, either suspended in solvents or made into a porous film. Nanostructured materials with the crystallite/grain size below 20nm are of great research interest mainly due to the fact that

their physical properties may be markedly different from the bulk counter parts. This has also opened up avenues for their applications as photocatalyst in numerous areas (Ameen *et* al., 2012). Generally, for all catalyst materials, a high surface area is an advantage in terms of a greater concentration of active sites per square meter and this generally leads to higher reactivity. The smaller the particle size, the larger the surface area, and the higher the expected activity (Ibhadon and Paul, 2013).

e. Size and Structure of the Photocatalyst

Surface morphological features such as particle size and structure are an important factor to be considered in photocatalytic degradation process because there is a direct relationship between organic compounds and surface coverage of the photocatalyst. The number of photons striking the photocatalyst controls the rate of reaction which signifies that the reaction takes place only in the absorbed phase of the photocatalyst (Zhu *et al*., 2006). Amor *et al*. (2018) reported SEM photographs of Zn–Al LDH and Zn-Al-Ti LDHs, The morphological features of LDHs showed non-uniform distribution. Furthermore, the images showed that all samples were agglomerated and possessed large and lumpy particles.

1.3.4 Application Of Photocatalysis

Applications of photocatalytic processes are widely recognized as viable solutions to environmental problems (Blake *et al.*, 1999).

Disinfection of bacteria is of particular importance, because traditional methods such as chlorination are chemical intensive and have many associated disadvantages. For example, in

water treatment applications, chlorine used for disinfection can react with organic material to generate chloro-organic compounds that are highly carcinogenic (Kool *et al.,* 1985).

a. Application of photocatalysis in water treatment

Growth in the global population, the diminishing supply of clean water, heightened environmental concerns, and the strong link between water quality and human health require the identification and employment of effective sustainable water treatment method to meet the urgent global need for clean water. Advanced oxidation processes (AOPs) have shown tremendous promise in water purification and treatment, including for the destruction of naturally occurring toxins, contaminants of emerging concern, pesticides, and other deleterious contaminants. One of the first references to AOPs was by Glaze in 1987 as processes that involve the generation of hydroxyl radicals in sufficient quantity to affect water purification. The definition and development of AOPs have evolved since the 1990s and include a variety of methods for generating hydroxyl radical and other reactive oxygen species including superoxide anion radical, hydrogen peroxide, and singlet oxygen. However, hydroxyl radical is still the species most commonly tied to the effectiveness of AOPs. Most organic compounds react with hydroxyl radical by addition or hydrogen abstraction pathways to form a carbon-centered radical. The resulting carbon-centred radical reacts with molecular oxygen to form a peroxyl radical that undergoes subsequent reactions, ultimately producing a host of oxidation products such as ketones, aldehydes and alcohols (Al-Rasheed *et al*., 2005).

b. Application in Indoor Air and Environmental Health

The photocatalytic process is well recognized for the removal of organic pollutants in the gaseous phase such as volatile organic compounds (VOCs), having great potential applications to

contaminant control in indoor environments such as residences, office buildings, factories, aircrafts, and spacecrafts (Tompkin *et al.,* 2005).

c. Biological and Medical Applications

Due to the disinfection abilities of photocatalytic processes, they are being explored for use in medical applications. Studies have been done using TiO_2 coatings on bioimplants to implement photocatalysis for antibacterial purposes, the outcome is photocatalysis was used in antibacterial activities (Lee *et al.* 2003).

d. Laboratory and Hospital Applications

Particularly, in microbiological laboratories and in areas in intensive medical use, frequent and thorough disinfection of surfaces is needed in order to reduce the concentration of bacteria and to prevent bacterial transmission. Conventional methods of disinfection with wiping are not long-term effective, and are staff and time intensive. These methods also involve the use of harsh and aggressive chemicals. Disinfection with hard ultraviolet light (UV) is usually unsatisfactory, since the depth of penetration is inadequate and there are occupational health risks (Kuhn *et al.,* 2003).

e. Pharmaceutical and Food Industry

Due to the antibacterial applications of TiO_2-mediated photo oxidation, this process shows promise for the elimination of microorganisms in areas where the use of chemical cleaning agents or biocides is ineffective or is restricted by regulations, for example in the pharmaceutical and food industries (Skorb *et al*., 2008). TiO_2 is nontoxic and has been approved by the American Food and Drug Administration for use in human food, drugs, cosmetics, and food contact materials (Chawengkijwani *et al*., 2008).

f. Plant Protection Applications

Photocatalytic disinfection is potentially very important in the control and inactivation of pathogenic species present in the nutritive solution in circulating hydroponic agricultures (Blanko *et al.,* 2009). Many plant pathogens can be transmitted by irrigation and recycled waters used in hydroponic agriculture. Conventional bactericidal methods often apply chemical pesticides to disinfect these pathogens, but these are often harmful to animals, humans, and the environment due to their residual toxicity (Yao *et al.,* 2007). Photocatalytic disinfection of these plant pathogens using TiO_2 may be used as a new tool for plant protection and an alternative to the use of harsh chemicals.

g. Wastewater and Effluents

The use of photocatalysis for water and wastewater treatment is a topic well documented in the literature, especially with respect to solar photocatalysis (Goswami and Blake 1996). Due to the ability of photocatalysis to mineralize many organic pollutants, it has been used for remediation of contaminated groundwaters through the use of parabolic solar concentrating type reactors. Photocatalysis has been used in engineering scale for solar photocatalytic treatment of industrial non biodegradable persistent chlorinated water contaminants (Malato *et al*., 2007), and in field scale for treatment of effluents from a resins factory (Turchi *et al.,* 1989).

1.3.5 Semiconductor Photocatalysis

Semiconductors used for the photocatalytic degradation of organic molecules are usually metal oxides or metal sulfides. The most commonly studied semiconductors include TiO_2, ZnO, WO_3, Fe_2O_3, and ZnS (Sun and Pignatello, 1995). In searching for an ideal photocatalyst for remediation of organic molecules using sunlight, several factors must be taken into account; chief among them are oxidation potential and energy of the band gap. The oxidation potential is important, since the ability to form photogenerated valence band holes (h^+_{vb}) and to create

hydroxyl radicals ($HO^{\bullet}$ ads) in water is key to its use as a photocatalyst for the oxidation of organic molecules. This is also true of the reducing power of the excited conduction band electron (e^{-}_{cb}), which must be of sufficient energy to reduce molecular oxygen to superoxide (Mills *et al.*, 1994). These two chemical processes are the key to the photocatalysis of organic molecules to simple gaseous products (H_2O, CO_2) and inorganic ions (NO_3^-, $SO4^{2-}$).

1.3.6. Activated Carbon as Support for Photoacatalyst

Carbons are strong light absorbing materials, despite of which they have been successfully used as support of photoactive species (Keller *et al*., 2005). Enhancing the photodegradation process and photon energy in its initiation of electron photo excitation and generation of radical. Activated carbon support has been used and reported as more promising in photo degradation of pollutants (Minero *et al*., 1992; Matos *et al*., 1989). A mixture of activated carbon and semiconductors has been reported to have a synergistic effect on the photodegradation of organic pollutants (Colon *et al*., 2003; Arana *et al*., 2003). Porosity of activated carbon leads to high adsorption of pollutants on the catalyst surfaces, which might accelerate the process of decomposition through the transfer of the adsorbed pollutant to the catalyst active sites. carbon-semiconductors composites have shown quite high efficiencies for the photodegradation of a variety of pollutants (Zhang *et al*., 2006). For instance, the presence of activated carbons and carbon nanotubes seems to change the photocatalytic activity of semiconductors towards the degradation of organic pollutants beyond the so-called “synergistic” effect (i.e., improved photodegradation rates). Here, carbon materials have been mainly used as supports of the photoactive species in the catalytic degradation of pollutants, and the synergistic effect observed in carbon-supported catalysts has been linked to the decrease in the recombination rate of the hole/electrons pair generated in the semiconductor when immobilized (Zhang *et al*., 2006). In

this research work 83.80% was achieved in the photodegradation of Methyl red using Cd-Al/AC catalyst

1.3.7 Mechanism Of Photocatalysis

Firstly, when a Cd-Al/AC and Cd-Sb/AC LDHs molecule absorbs a photon with energy equal to or larger than its band gap, the excited electrons of LDH material were promoted from the valence band to the conduction band yielding holes (h^+) and photon generated electrons (e^-) (Rauf *et al.*, 2007).

$$\text{Catalyst} + hv \rightarrow e^-_{cb} + h^+_{vb} \quad \text{.....(2)}$$

The electron hole h^+ react with water to produce $^{\cdot}OH$ photo generated e^- react with dissolved oxygen to produce superoxide radical anion of oxygen (Mahmoodi *et al*., 2006).

$$H_2O + h^+_{vb} \rightarrow {}^{\bullet}OH + H^+ \quad \text{.....(3)}$$

$$O_2 + e^-_{cb} \rightarrow O_2^{-\cdot} \quad \text{.....(4)}$$

This reaction prevents the combination of the electron and the hole which are produced in the first step. The $^{\bullet}OH$ and $O_2^{-\cdot}$ produced in the above are responsible for the oxidation of the organic molecule producing degradation products.

$$O_2^{-\cdot} + H^+ \rightarrow HOO^{\cdot} \quad \text{.....(5)}$$

$$2HOO^{\cdot} \rightarrow H_2O_2 + O_2 \quad \text{.....(6)}$$

$$H_2O_2 \rightarrow 2HO^{\cdot} \quad \text{.....(7)}$$

$$OH^{\cdot} + \text{dye} \rightarrow \text{Degradation product} \quad \text{.....(8)}$$

1.4 LAYERED DOUBLE HYDROXIDE (LDH)

Chemical composition of LDH (Fig. 1) is generally expressed as $(M^{(II)}_{1-x} M^{(III)}_{x} (OH)_2)^{x+} A^{n-} x/n .yH_2O$, where, $M^{(II)}$ =divalent cation, $M^{(III)}$ =trivalent cation, A =interlayer anion, n=charge on interlayer ion, and x and y are fraction constants. Inorganic or organic anions can be introduced between hydroxide layer by ion exchange or precipitation (Sung *et al*., 2001).

Considered generally as promising materials in view of their high chemical versatility associated with a tunable anionic exchange capacity, LDHs are widely used in commercial products as catalysts, adsorbents, anion exchangers, acid residue scavengers, flame retardants and polymer stabilizers (Choi and Choy 2008). Due to the highly active surface atoms, LDH powders are spontaneously ready to aggregate during storage and application, thus leading to limitations in their technical applicability. Therefore, it is of great interest and importance to generate alternative predefined structures.

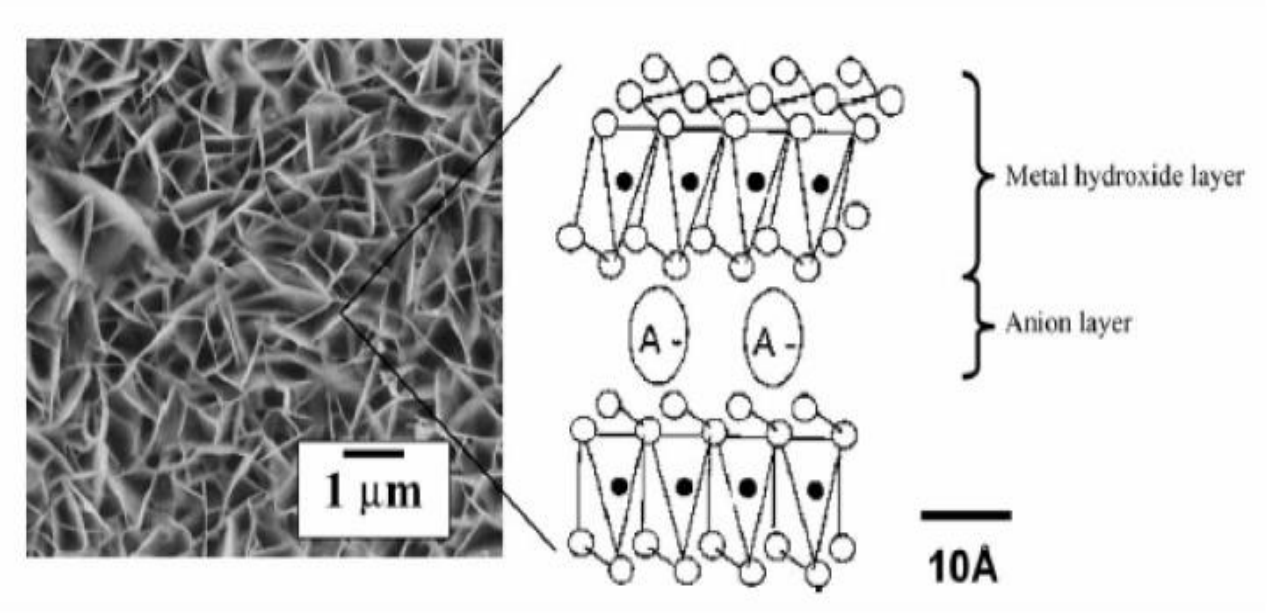

Figure. 1.1 - A schematic illustration of LDHs structure (Metal hydroxides layer located on top and bottom layers while anion layer located in middle (Wong *et al*., 2004).

1.4.1 Preparation of Layered Double Hydroxides (LDHs)

Several methods are currently available for the production of LDHs. The main methods are explained belows.

a. Reconstruction Method

Metal salts are calcined at 500°C for 4 h in nitrogen at a heating rate of 5°C/min. This solid is then added to solution containing decarbonated water with guest molecule. pH (7-8)is adjusted by NaOH. Then, the precipitate was aged at room temperature, filtered, washed with decarbonated water thoroughly and finally dried under vacuum (Jung *et al*., 1996).

b. Co-precipitation Method

Typically, a mixed solution of two different metal salts in decarbonated water is added dropwise over one hour to an aqueous solution containing organic guest species under nitrogen atmosphere with vigorous stirring. During titration, solution pH (7-8) is adjusted with 0.1 N

NaOH to induce co-precipitation. Then the precipitate was aged at room temperature for 24 h, is filtered, washed with decarbonated water thoroughly and finally dried under vacuum (Jung *et al.*, 1996). LDH hybrids can be prepared by ion-exchanging interlayer anion of LDH with biomolecules. Co precipitation method is more useful (yield, 3 times) than reconstruction method (Jung *et al.*, 1996).

c) Salt-oxide Method

In this method, a bivalent metal oxide suspension is reacted with a trivalent metallic cation solution and the anion to be intercalated. The pH should be kept slightly acidic to occur slow hydrolysis of the divalent cation oxide. This method has some requirements, such as, the need for the divalent cation oxide undergoes slow hydrolysis and the anion to be intercalated must be able to form a soluble salt with the trivalent cation and be stable in acidic medium (Boehm *et al*., 1977).

d) Hydrothermal Synthesis Method

The hydrothermal synthesis method use suspension of oxides and/or hydroxides of M^{2+} and M^{3+} cations. Into this suspension, it is inserted a solution with acid or salt. The reaction occurs at high pressure and temperature. The great advantage of this method, when compared with coprecipitation, is to avoid undesirable waste discard, which may be harmful to the environment, such as NO^{-3}, Cl^{-}, OH^{-} , etc (Wang *et al*., 2013).

e) Induced Hydrolysis Method

It consists of the precipitation of M^{3+} cation hydroxide at pH slightly below that in which M^{2+}

cation hydroxide precipitation occurs. The aqueous suspension of M^{3+} is added into the M^{2+} one, maintaining pH at a fixed value by simultaneous addition of a NaOH solution (Taylor *et al*., 1984).

f) Sol-Gel Method

In this method, the reaction occurs in an alcohol solution of magnesium ethoxide dissolved in HCl with a solution containing Al tri-sec-butoxide. The mixture is heated to reflux and stirred until gel formation. The material prepared by this method has controlled pore size and high specific surface area. The sol-gel method has been used in LDH synthesis as it has a great advantage of producing materials with higher purity (Wang *et al*., 1999).

1.4.2 Properties of Layered Double Hydroxides (LDHs)

LDH present a great number of properties due to their varied compositions and methods of synthesis.

a) Anion Exchange Capacity

For LDHs, the Anion Exchange Capacity (AEC) depends on the metallic cation ratio, the ability of the involved anion in stabilizing lamellar structure and molecular mass of the cations and anions involved (Leroux and Besse, 2004).

b) Colloidal Properties

The small particle size and low charge density of some LDH are important for systems with colloidal characteristics and delamination (stacking structure loss). The large size of the host anion often cause interlayer diffusion problems. Thus, in order to overcome these problems, colloidal and delaminated systems, which are formed from LDH, allow a better arrangement of the lamellae between host and anion. Several studies have reported the formation of systems with

colloidal features by combining LDH and organic molecules (Zhao *et al*., 2002; Leroux and Besse, 2004).

c) Morphological Properties

Physical properties such as morphology, surface area, porosity and particle size are extremely important to describe LDH and, of course, can define its applications. Conventional preparation methods of LDH provide limited control over these properties. Scanning Electron Microscopy (SEM) can be used to assess the morphology of these materials (Leroux and Besse, 2004).

d) Thermal Stability

Thermal stability is another important property of LDH. Thermal characterization of LDH materials is performed by Thermogravimetric Analysis (TGA) and Differential Scanning Calorimetry (DSC) techniques. Thermal decomposition temperatures are dependent on several factors such as, LDH crystallinity, nature, cations molar ratio (M^{2+}/M^{3+}), and the interlayer anion type (organic or inorganic). When organic anions are within LDH layers, resulting in intercalated nanomaterials, it usually shows higher thermal stability relatively to the free organic anion. Some researchers have speculated that the nature of organic and inorganic component interface is the reason for thermal stability improvement. Another hypothesis is that LDH may act as a protective layer, delaying the byproduct crystallization and inducing unusual solid formation after heat treatment under inert atmosphere (Leroux and Besse, 2004). The thermal decomposition of LDHs usually occurs as a two-step process. The first stage in the decomposition process is dehydration of the interlayer water molecules. This loss occurs around 187^{o}C (460 K), and results in a water free LDH. In the second stage, which occurs in the range of

380^{o}C (653 K), the clay starts to dehydroxylate and the interlayer anion decomposes (Hongbo et al., 2015).

1.5 DYES

Dyes are intensely colored, soluble substance giving a clear solution and can be applied in solutions or dispersions to textiles, paper or gelatin layer in photographic film and paper, leather fur, etc., to give a colored material considerable fastness (Popoola, 2015). There are different dyes that are available for commercial use such as; disperse, basic, azo, diazo, acidic, anthraquinone based and complex metal based dyes. About 10,000 different dyes are prepared globally, and approximately 8×105 tons of synthetic dyes is consumed in textile industries in the whole world (Demirbas, 2009).

1.5.1 Classification of Dyes

Dyes may be classified according to their chemical structure or by their application method.

a. Chemical classification is the classification of dyes by their chemical structure. The classification of dyes that emerged based on the basis of chemical structure was found more or less to be that of available chromophore for example azo dyes (-N=N-) (strong, good all-round properties and cost-effective) example Methyl red and anthraquinone dyes ($C_{14}H_8O_2$) (weak, expensive) example Pigment yellow 108 (Popoola, 2015).

b. Usage classification i.e the classification of dyes by its use or method of application, e.g., dispersed dyes which have low solubility in aqueous solution (Popoola, 2015).

1.5.2 Types of Dyes

Dyes are also broadly categorized into two groups;

1) Natural dyes

2) Synthetic dyes

1) Natural Dyes

Natural dyes are organic compounds used to color various products. Before the year 1865, natural dyes are extracted from plants, animals, insects and mineral sources (Popoola, 2015). Natural dyes are such as Turmeric, Weld, Onion, Jackfruit, henna, eucalyptus are used in the early textile industry. Due to the increased industrial activities, natural dyes do not meet the industrial demand, and their applications have been limited mainly to food industries (Popoola, 2015).

2) Synthetic Dye

The first synthetic dye (aniline purple) was discovered accidentally by Williams Henry Perkin in 1856. Dye effluents are produced because dyes do not have a complete degree of fixation to the fiber during dyeing and finishing processes (Pang and Abdullahi 2013).The various types of synthetic dyes used in industries are acid dyes, reactive dyes, basic dyes, azo dyes, direct dyes, vat dyes and disperse dyes (Demirbas, 2009). Disperse and vat dyes are not soluble in water. All dyes contain traces of metals such as copper, zinc, lead, chromium and cobalt in their aqueous solution except vat and disperse dyes. The synthetic dyes are for the classified as explained below.

a. Cationic (basic) Dyes

Cationic (basic) dyes are water-soluble dyes applied to paper, polyacrylonitrile (e.g. dralon), modified nylons and modified polyesters (Hunger, 2003).They reported that the original use of this group of dyes was for wool, silk, and tannin-mordanted cotton when brightness is

germane than fastness to light and washing. They yield colored cations in solution, and this is the reason for calling them cationic dyes. The principal chemical classes of basic dyes are Triphenylmethane, Thiazine, Oxazine, and Acridine. Examples of basic dyes are Malachite Green and Crystal Violet.

b. Acid Dyes

Acid dyes are water soluble anionic dyes carrying the organic sulphonic acid group. However, their commercially available forms are usually sodium salts which exhibit excellent water solubility property (Turabik 2008). They are applied to nylon, wool, paper, leather, food, cosmetics, etc. Most synthetic food colors fall in this category. The principal chemical classes for these dyes are Azo, Anthraquinone, Nitro, Nitroso, Xanthene and Azine. Examples are Acid Yellow, Acid Blue (Demirbas, 2009).

c. Vat Dyes

Vat dyes are water insoluble and incapable of dyeing fibers directly. But, reduction in alkaline liquor produces the water soluble alkali metal salt of the dye, which, in this leucophores, has an affinity for the textile fiber. They are used to dye cellulosic. They are used for Rayon, Wool, Cotton, and Nylon. They fall under the major class containing Anthraquinone and indigoid. An example of vat dye is Caledon Golden Yellow (ICI), C.I. Vat Orange 9(59700) (Demirbas, 2009).

d. Disperse Dyes

Disperse dyes are substantially water soluble nonionic dyes for application to hydrophobic fibers from an aqueous dispersion. They are a heterogeneous collection of several chemical types, but the anthraquinone and azo groups are the primary chromophoric system

present in disperse dyes. These are used mainly on polyester and also applied on nylon, cellulose, acrylic fibers, etc. They contain Styryl, Nitro, and Benzodifuranone (Demirbas, 2009).

e. Reactive Dyes

Reactive dyes form a covalent bond with the fiber and contain chromophore groups such as Azo, Anthraquinone, Triaryl methane, Phthalocyanine, Formazan, Oxazine, etc. They have simpler chemical structures; their absorption spectra show narrow absorption bands and the dyeing are brighter making them have an edge over direct dyes. Reactive dyes are used for cotton and other cellulosic but are also used to a small extent on wool and nylons (Demirbas, 2009).

f. Anionic-Direct Dyes

These are water soluble anionic dyes when applied from the aqueous medium in the presence of an electrolyte; it has a high affinity for cellulosic fiber. Their principal use is in the dyeing of cotton and rayon, paper, leather, and to some extent to nylon. Most of the dyes in this class are polyazole compounds, along with some Stilbenes, Phthalocyanines, and Oxazines (Demirbas, 2009).

g. Sulphur Dyes

These dyes have intermediate structures. Dyes in these groups are applied by the vat technique mainly on cellulosic fiber. They are temporarily solubilized dyes which are converted to water soluble reduced forms in sodium sulfide bath for the purpose of impregnation into the fabrics. After impregnation the dye is re-oxidized to its insoluble form by exposure to air, dyed article usually in black, green, blue and brown shades have good wet fastness properties (Demirbas, 2009).

h. Solvent Dyes

Solvent dyes are water soluble and nonpolar. They have non-solubilizing groups such as -SO_3H- or-CO_2H- which will make them applicable in an aqueous medium. However, they are soluble in various organic solvent ranging from alcohols, esters, ketones, hydrocarbon solvents and oils. They are used in manufacturing biological stains, lacquers and also as pigmentation Compounds in coloring candles, cosmetics, polishes, surface finishes, soaps and also as a host of other applications (Demirbas, 2009).

i. Condense Dyes

They are dyes whose molecules on application react with each other or with the molecules of another compound to form larger sized molecules (Demirbas, 2009).

j. Mordant Dyes.

These dyes use a mordant, which improves the fastness of the dye against water, light, and perspiration. The choice of mordant is very vital as different mordants can change the final color significantly. These are used for wool (Demirbas, 2009).

1.5.3 Methyl Red Dye

Methyl Red (2-(N,N-dimethyl-4-aminophenyl) azobenzenecarboxylic acid) also called C.I Acid Red 2, is an indicator dye that turns red in acidic solutions. It is an azo dye and is a dark red crystalline powder. Methyl red is a pH indicator that appears red in pH under 4.4, yellow in pH over 6.2 and orange in between, with pka value of 5.1 (Kubin 1982). Preferred IUPAC 2-{[4-(Dimethylamino)phenyl]diazenyl}benzoic acid. The properties of this dye are as follows.

Properties of Methyl Red

Chemical formular: $C_{15}H_{15}N_3O_2$

Molar Mass: 269.304 g,mol^{-1}

Density: 0.791 g/cm^3

Melting Point: 179-182^{o}C

λ_{max}: 463nm

Refractive index: 1.5930

Stability: Stable, incompatible with strong Oxidizing agents.

Solubility: Soluble in glacial, acetic acid, benzene, and ethanol.

Insoluble in water.

Flash Point: 11^{o}C

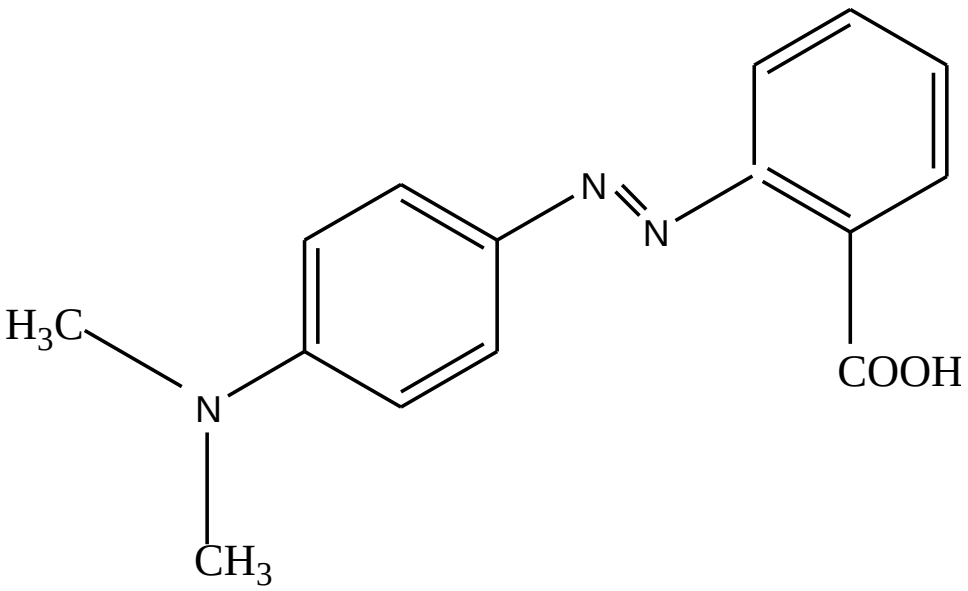

Structure/Figure 1.2: Chemical structure of Methyl Red (Adowei *et al*., 2012)

1.5.4 Rhodamine B

Rhodamine B is a dye. It is often used as a tracer dye in water the rate and direction of flow and transport. Rhodamine B dyes fluoresce and thus be detected easily and inexpensively with fluorometers. Rhodamine B dyes are used extensively in industry. The IUPAC name for dye is [9-(2-carboxyphenyl)-6-diethylamino-3-xanthenylidene]-diethylammonium chloride

It comparised of the following Properties

Chemical formula; $C_{28}H_{31}CIN_2O_3$

Molar mass: 479.02

Melting Point: 210 to 211^{O}C

λ_{max}: 554nm

Solubility Approximately: 15g/L (20^{O}C)

Refractive index: 1.6500

Stability: Stable, incompatible with strong Oxidizing agents.

Flash Point: 12^{o}C (Kubin 1982)

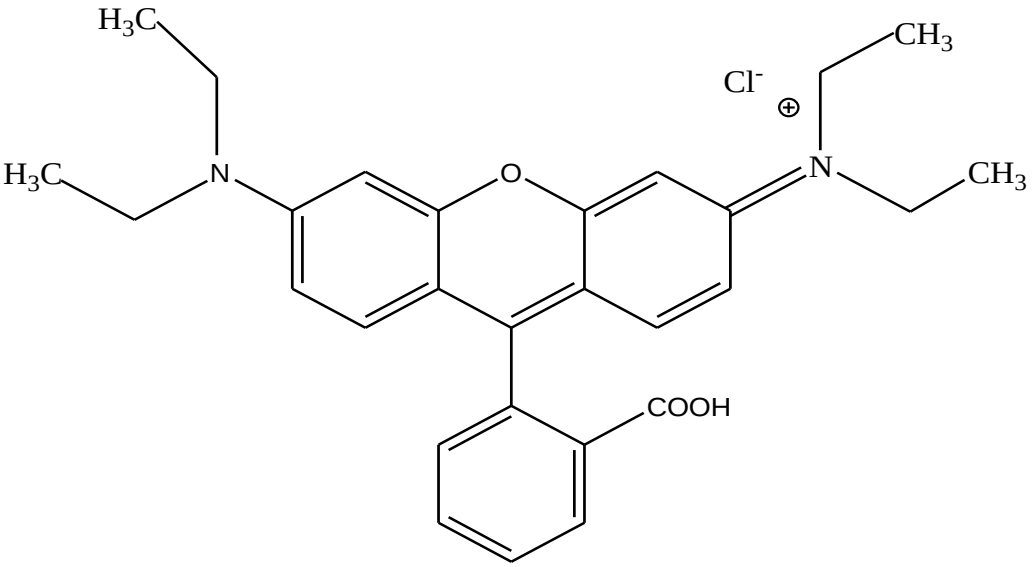

Structure/Figure 1.3: Chemical structure of Rhodamine B (Inyinbor *et al*., 2015).

1.6 Aim and Objectives of the study

The aim of this research is to determine the efficiency of two different catalysts (i.e. Cd-Al/AC and Cd-Sb/AC) in the degradation of RB and MR under visible light, as possible alternative for wastewater treatments.

The specific objectives of the research work are as follows:

1. To synthesize of Cd-Al/AC and Cd-Sb/AC layered double hydroxide catalysts using co-precipitation method.
2. To characterize Cd-Al/AC and Cd-Sb/AC layered double hydroxide catalysts using X-ray Diffaraction (XRD), Scanning Electron Microscopy (SEM) and Fourier Transform Infrared Spectroscopy (FT-IR).
3. To study the effect of the Cd-Al/AC and Cd-Sb/AC catalysts in the photocatalytic degradation of RB and MR.
4. To determine the band gap energy of synthesized Cd-Al/AC and Cd-Sb/AC LDHs.

5. To carefully monitor and interpret the kinetics of photocatalytic process involving the two catalysts.

1.7 Scope and Limitation of the Study

The research was limited to the preparation, characterization and study of photocatalytic properties of Cd-Al/AC and Cd-Sb/AC for the removal of dyes (Rhodamine B and Methyl red). Characterization of the prepared catalyst was carried out using X-ray Diffaraction (XRD), Fourier Transform Infrared (FT-IR) Spectroscopy and Scanning Electron Microscopy (SEM)

1.8 Statement of the Research Problem

Among the several hazardous compounds that are found in water, dyes are an important class of concern. The treatment of colored wastewater not only involves its decolorization, but also its detoxification. Textile and similar other industries release large amounts of colored dye effluents into the water. These dye effluents are toxic and many of them are non-biodegradable. These effluents create major environmental problems and release potentially harmful carcinogenic substances in water. It has become necessary for us to develop an efficient, cost effective and environmentally friendly technique in order to reduce or to minimize it to the minimum level possible. However several method that are used in the photodegradation and mineralization of these organic dyes ware found to be ineffective due to the formation of secondary waste product but photocatalysis is being considered as an efficient process for the mineralization of toxic organic compounds, due to the generation of hydroxyl radicals (OH•) which possess strong oxidizing potential. However, researches involving the photodegradation of Rhodamine B and Methyl red using Cd-Al/C and Cd-Sb/C layered double hydroxides as catalysts due to their high anion exchange capacity have not been reported.

CHAPTER TWO

2.0 LITEREATURE REVIEW

2.1 Photocatalysis Using Semiconductors Catalysts

Jean (1999) reported that Photocatalysis is based on the double aptitude of the photocatalyst (TiO_2) to simultaneously adsorb both reactants and to absorb efficient photons. The basic fundamental principles are described as well as the influence of the main parameters governing the kinetics (mass of catalyst, wavelength, initial concentration, temperature and radiant flux). Besides the selective mild oxidation of organics performed in gas or liquid organic phase, UV-irradiated titania becomes a total oxidation catalyst once in water because of the photogeneration of $OH^{\cdot}$ radicals by neutralization of OH^{-} surface groups by positive photo-holes. A large variety of organics could be totally degraded and mineralized into CO_2 and harmless inorganic anions. Any attempt of improving TiO_2 photo activity by noble metal deposition or ion-doping was detrimental. In parallel, heavy toxic metal ions (Hg_2C, AgC, noble metals) can be removed from water by photo deposition on TiO_2. Several water -detoxification photocatalytic devices have already been commercialized. Solar platforms are working with large-scale pilot photo reactors, in which are degraded pollutants with quantum yields comparable to those determined in the laboratory with artificial light.

Hussein *et al.* (2007) reported the photodegradation of a real textile dyeing wastewater obtained from Hilla textile factory in Babylon Governorate, Iraq. Photocatalytic degradation was carried out over suspensions of TiO_2 or ZnO under ultraviolet irradiation. Photodegradation percentage was followed spectrophometrically by the measurements of absorbance at λmax equal to 380 nm. The rate of photodegradation increased linearly with time of irradiation when TiO_2 or ZnO was used. A maximum color removal of 96% was achieved after irradiation time of 2.5

hours when TiO_2 used at 303K and 82% color reduction was observed when ZnO used for the same period and at the same temperature. The effect of temperature on the efficiency of photodegradation of dyestuff was also studied. The activation energy of photodegradation was calculated and found to be equal to 21 ± 1 kJ mol^{-1} on TiO_2 and 24 ± 1 kJ mol^{-1} on ZnO.

Hameed and Akpan (2009) investigated the effects of operating parameters on the photocatalytic degradation of textile dyes using TiO_2-based photocatalysts. It further examines various methods used in the preparations of the considered photocatalysts. The findings revealed that various parameters, such as the initial pH of the solution to be degraded, oxidizing agents, temperature at which the catalysts must be calcined, dopant(s) content and catalyst loading exert their individual influence on the photocatalytic degradation of any dye in wastewaters. It was also found out that sol–gel method is widely used in the production of TiO_2-based photocatalysts because of the advantage derived from its ability to synthesize nanosized crystallized powder of the photocatalysts of high purity at relatively low temperature.

Jimin *et al.* (2009) used a series of rare earth (Sm^{3+}, Nd^{3+}, Ce^{3+} and Pr^{3+}) doped TiO_2-SiO_2 photocatalysts, as a reclaimed solar-light responsive photocatalyst, was prepared by sol–gel method with tetraethoxysilane (TEOS) and tributylin (TBT) as precursors, by keeping the molar ratio of TEOS:TBT constant at 1:1 and with different rare earth dopant content. The photocatalysts were characterized by X-ray diffraction (XRD), transmission electron microscope (TEM), scanning electron microscope (SEM), energy dispersive spectroscopy (EDX), UV–vis diffuse reflectance, Fourier transform infrared spectra (FTIR) and nitrogen adsorption/desorption isotherms. The characterizations found that only anatase phase was present in photocatalysts with high surface area. The mean size was around 10.1nm from TEM, which is consistent with the analytical result according to SEM. It can be seen that methyl groups exist in photocatalysts

based on analysis of FTIR. The distinct band for Ti–O–Si vibration (~970cm^{-1}) is observed as indicated from FTIR. Comparing to undopedTiO_2-SiO_2 photocatalyst, the rare earth doped TiO_2-SiO_2 photocatalysts exhibit obvious absorption in the 400–450nm range with a red shift in the band gap transition. The experiments also confirmed that TiO_2-SiO_2 photocatalysts with rare earth ions dopant content increase the efficiency of interfacial adsorption and photocatalytic reactivity on the degradation of methylene blue (MB, 10 mg/L) in water under solar-light irradiation. Meanwhile, the rare earth doped TiO_2/SiO_2 photocatalysts remained floatable in the water surface after irradiation for 3 h. The solar-light driven photocatalysts with low preparation can be easily scaled up for industrial application, especially in the open water surface. The photocatalytic effects of the samples were evaluated by the extent of decolorization of MB in an aqueous solution. In a typical experiment, a 100mL of MB solution (concentration: 10 mg/L) was placed in the beaker and the photocatalysts were added to the MB solution. The amount of the photocatalyst is equivalent to 100mg of TiO_2. Prior to irradiation the catalyst was immersed into the solution in darkness for 30 min to ensure adsorption/desorption equilibrium, then the solutions were exposed to sunlight at room temperature with constant stirring.

Cooper *et al.* (2013) reported that a cross-section of TiO_2 compositions for which existing evidence suggests the prospect of improved performance compared to standard Degussa P25. In the context of a program aimed toward a 365 nm LED based photo-reactor, the question is whether a distinctly superior photocatalyst composition for drinking water treatment is now available that would shape and design choices. An answer was sought by synthesizing several photocatalysts with reported high reactivity in some context in the literature, and by performing photocatalysts reactivity tests using common pollutants of water system including Natural

Organic Matter (NOM) and Emerging Contaminants (ECs) from the pesticide and pharmaceutical classes. 365 nm Light Emitting Diodes (LEDs) were used as the irradiation source. Since LEDs are now available in the UV, we did not examine the TiO_2 modifications that bring band gap excitation into the region beyond 400 nm. The results suggest that the choice of the photocatalyst should be best made to fit the reactor design and photocatalyst mounting constraints such as mass transport, reactive surface and light field

El-Sayed *et al.* (2014) reported that various destructive Mg/Al layered double hydroxide (LDH)-Titanium photocatalysts were prepared using different strategy. TiO_2/LDH mechanical mixture catalyst was obtained by kneading various mass ratios. TiO_2/LDH Core Shell catalyst was obtained by coprecipitating LDH salts on TiO_2. Ti_4^+-functionalized Mg/Al LDH (Ti-LDH) in which LDH metals might be replaced by Ti using $TiCl_4$. Mg/Al/Ti LDH Catalysts in which titanium might be incorporated into LDH lattice structure was prepared using $TiCl_4$. The catalysts were characterized using several techniques such as, XRD, TEM/EDS, SEM to investigate their crystallinty and surface morphology. The band gab was determined using UV-VIS defused reflectance. The photocatalytic efficiency of catalysts was evaluated for removal of phenol under UV irradiation. The effect of mass ratios of the mechanical mixture has been investigated. All catalysts manifest better phenol removal and better Separation from samples than TiO_2 itself. In the Core Shell catalyst, TiO_2 photo sensitive surface might be much closer to the hydroxide groups of LDH, which might explain the higher percent removal of phenol than the others. The photocatalytic efficiency of the mixture was decreased by increasing LDH weight ratio, it might due to decreasing photo sensitive surface of the catalyst mixture, the highest efficiency they have achieved was 85% using 1:1 TO_2:LDH molar ratio.

Ahmad *et al.* (2014) reported that Rhodamine B (RB) is a toxic dye used extensively in textile industry, which must be remediated before its drainage to environment. In their study, supported gold nanoparticles on commercially available titania and zincite were successfully prepared and then their activity on the photodegradation of RB under UV light irradiation was evaluated. The synthesized photocatalysts were characterized by ICP, BET, XRD, TEM and EDX. Kinetic results showed that Au/TiO_2 was a photocatalyst inferior to Au/ZnO. This observation could be attributed to the strong reflection of UV irradiation by gold nanoparticles over TiO_2 support.

Sriparna *et al*. (2014) reported an aligned array of hydrothermally grown, multi walled hydrogen titanate ($H_2Ti_3O_7$) nanotubes anchored to both faces of a metallic Ti foil acts as an efficient photocatalyst. We studied the degradation of rhodamine B dye in the presence of the nanostructured photocatalyst under UV irradiation, by monitoring the optical absorption of the dye. Rhodamine B was chosen as a representative and particularly harmful industrial pollutant dye. The inner and outer diameters of the $H_2Ti_3O_7$ nanotubes were 5nm and 10 nm, respectively. The nanotube array catalyst is recyclable and structurally stable. Most importantly, it shows comparable or higher photodecomposition rate constant than those of both $H_2Ti_3O_7$ nanotube powder and P-25 (Degussa). The enhanced photocatalytic performance may be ascribed to the nanotube array having a super hydrophilic surface with a high accessible surface area.

Zhang *et al.* (2016) reported Magnetic FeO/Fe_3O_4/graphene has been successfully synthesized by a one-step reduction method and investigated in rapid degradation of dyes in this work. The material was characterized by N_2 sorption–desorption, scanning electron microscopy (SEM), Fourier transform infrared spectroscopy (FT-IR), vibrating-sample magnetometer (VSM) measurements and X-ray photoelectron spectroscopy (XPS). The results indicated that

FeO/Fe_3O_4/graphene had a layered structure with Fe crystals highly dispersed in the interlayers of graphene, which could enhance the mass transfer process between FeO/Fe_3O_4/graphene and pollutants. FeO/Fe_3O_4/graphene exhibited ferromagnetism and could be easily separated and re-dispersed for reuse in water. Typical dyes such as Methyl Orange, Methylene Blue and Crystal Violet could be decolorized by FeO/Fe_3O_4/grapheme rapidly. After 20 min, the decolorization efficiencies of methyl orange, methylene blue and crystal violet were 94.78%, 91.60% and 89.07%, respectively. The reaction mechanism of FeO/Fe_3O_4/graphene with dyes mainly included adsorption and enhanced reduction by the composite. Thus, FeO/Fe_3O_4/graphene prepared by the one-step reduction method has excellent performance in the removal of dyes from water.

Yong *et al.* (2017) reported novel FeAgPt alloy nanoparticles were biosynthesized via ultra-sonication using the root extract of Platycodongrandi florum. The nanoparticles exhibited enhanced catalytic activities in the reduction of 4-nitroaniline (4-NA) to p-phenylenediamine with a significantly reduced reaction time and increased rate constant because of their high number of active surface sites. In addition, the same catalyst exhibited enhanced catalytic activity in the decolorization of an environment polluting dye, Rhodamine B (RhB).

2.2 Photocatalysis Using Layered Double Hydroxide

Milica *et al.* (2010) reported that Layered double hydroxides (LDHs) and mixed oxides derived after thermal decomposition of LDHs with different Mg–Fe contents were investigated. These materials were chosen because of the possibility to tailor their various properties, such as ion-exchange capability, redox, acid–base and surface area. Layered double hydroxides, $[Mg_{1-x}Fe_x(OH)_2](CO_3)_{x/2}.mH_2O$ (where x presents the content of trivalent ions, $x = M^{(III)}/(M^{(II)} + M^{(III)})$ were synthesized using the low supersaturation precipitation method. The influence of different

Mg/Fe ratios on the structure and surface properties of the LDH and derived mixed oxides was investigated in correlation to their catalytic properties in the chosen test reaction (Fischer–Tropsch synthesis). It was determined that the presence of active sites in the mixed oxides is influenced by the structural properties of the initial LDH and by the presence of additional Fe phases. Furthermore, synthesis outside the optimal range for the synthesis of single phase LDHs leads to the formation of meta stable, multiphase systems with specific characteristics and active sites.

Carriazo *et al*. (2011) reported that Layered double hydroxides (LDH) containing zinc and aluminium within the brucite-like layers and carbonate as the interlayer anion have been used as precursors for the preparation of mixed metal oxides by calcination. ZnO and the $ZnAl_2O_4$ spinel were formed with different degree of crystallinity depending of two parameters, the Zn^{2+}/Al^{3+} molar ratio and the calcination temperature (500–800 ◦C) of the LDH precursor. A pure spinel phase was obtained to remove ZnO upon a basic post-treatment in NaOH solution of the samples calcined at 800 ◦C. All the samples were tested for the photodegradation of 2-propanol in gas–solid regime. All the samples resulted active as heterogeneous photocatalysts. The photocatalytic activity increased by increasing the Zn^{2+}/Al^{3+} molar ratio and the calcination temperature of the solids.

Meng-Qiang *et al*. (2010) investigated that a family of layered double hydroxides (LDHs), such as Fe/Mg/Al, Co/Mg/Al, and Ni/Mg/Al LDHs, were used as catalysts for the efficient growth of single-walled carbon nanotubes (SWCNTs) in a fluidized bed reactor. The LDH flakes were agglomerated into clusters with sizes ranging from 50 to 200 nm, and they can be easily fluidized with a gas velocity ranging from 2.3 to 24 cm/s. After calcination and reduction, small metal catalyst particles formed and distributed uniformly on the flakes. At the

reaction temperature, the introduction of methane realized the growth of SWCNTs with the diameter of 1–4 nm. The loose structure of LDH agglomerates afforded a yield as high as 0.95 gCNT/(gcat h) of SWCNTs with a surface area of 930 m^2/g. Compared with Fe/Mg/Al LDH, Ni/Mg/Al and Co/Mg/Al LDHs showed a better selectivity to SWCNTs. The highest selectivity for metallic SWCNTs was obtained using Co/Mg/AI LDHs as the catalyst.

Min *et al*. (2012) reported the oriented Cu–Cr layered double hydroxide (LDH) films have been fabricated by the electrophoretic deposition method (EPD) on copper substrates, which can be used as photocatalysts for the degradation of organic pollutants under visible-light irradiation. Powder X-ray diffraction (PXRD), scanning electron microscope (SEM), Fourier transform infrared (FT-IR) and Brunauer–Emmett–Teller (BET) reveal that the resulting CuCr-LDH film possesses high crystallinity, porous structure as well as large specific surface area. UV–vis diffuse reflection spectroscopy (DRS) confirms that the CuCr-LDH film shows a broad absorption in visible light region (>400 nm). The LDH film thickness can be controlled precisely by adjusting voltage or time of EPD. The film with thickness of 16.5 nm shows excellent photocatalytic activity for the degradation of 2,4,6-trichlorophenol (2,4,6-TCP), sulforhodamine B (SRB) and Congo red. The photocatalytic reaction kinetics of 2,4,6-TCP was appropriately described by the pseudo-first-order model. In addition, the LDH film exhibited excellent recycleability compared with the corresponding powder sample, which facilitates its repeatable and cyclic usage over a long period. Owing to the high efficiency, low-cost preparation, easy manipulation and recyclability, it is expected that this film can be potentially used as photocatalyst in the field of water treatment.

Shahid *et al.* (2016) investigated Cd-Al/C and Cd-Sb/C layered double hydroxides nanocatalyst for the decoloration and mineralization of organic dyes. These catalysts were largely characterized by FESEM, EDS, XRD, FTIR, XPS, PL and DRS. The diffuse reflectance data showed a band gap at 2.92 and 2.983 eV for Cd-Al/C-LDH and Cd-Sb/C respectively. The band gap suggested that both catalysts work well in visible range. The photoluminescence spectra indicated a peak at 623 nm for both the catalysts which further support the effectiveness of the respective catalyst in visible ranged. Both catalysts also showed good recyclability and durability till 4^{th} cycle. Five dyes, acridine orange (AO), malachite green (MG), crystal violet (CV), congo red (CR) and methyl orange (MO) were used in this experiment. Various parameters of different light intensity such as visible, ultraviolet, sunlight and dark condition are observed for the de-coloration of these dyes. The de-coloration phenomenon was proceeded through adsorption assisted phot-degradation. The low cost, abundant nature, good recyclability and better dye removal efficiency make these catalysts suitable candidates for the de-coloration and mineralization of organic dyes**.**

Ayawei *et al.* (2017) reported the ability of Mg/Fe- CO_3 to degrade Congo Red in aqueous solution under various experimental conditions. The layered double hydroxide was synthesized by co-precipitation method and characterized by X-ray diffraction (XRD), Fourier Transform Infrared spectroscopic (FTIR) and Energy- Dispersive X-ray Spectroscopic (EDX). Batch mode experiments were conducted to assess the potential of the layered double hydroxide for the removal of Congo red from aqueous solution. Laboratory experimental investigation was carried out to identify the effect of agitation time (10 - 30min), varying temperature (40-80˚C) and varying concentration (20 - 40m/L). The adsorption was endothermic and the computation of the parameters ΔG°, ΔH°, ΔS° and ΔH^{o} indicated that the interactions were thermodynamically

favorable. Langmuir, Freundlich, Temkin and the Dubinin–Kaganer–Radushkevich (DKR) adsorption isotherm models were used to qualify the experimental data with the best fits been Langmuir and Freundlich isotherms with regression coefficient values of 0.9995 and 0.9998 respectively.

Li *et al*. (2017) investigated that ZnO/NiO/$ZnAl_2O_4$ mixed metal oxides were synthesized through hydrothermal method in which solutions of appropriate amounts of metal salts were mixed with solutions of sodium hydroxide and sodium carbonate to obtain a series of hydrotalcite-like precursors. The precursors in the form of ZnNiAl layered double hydroxides (LDHs) were subject to calcination at suitable temperatures for the generation of composite oxides. The samples were characterized by XRD, SEM, TEM, EDS, BET and UV-Vis DRS techniques. The results indicate that there is the generation of well-crystalline ternary ZnO/NiO/$ZnAl_2O_4$ photocatalysts high in surface area. The photocatalytic activity of the materials was evaluated in the photocatalytic reduction of CO_2 under simulated sunlight irradiation. The effects of calcination temperature, amount of sacrificial agent and reaction time on the photocatalytic activity of the samples were investigated. The results indicated that ZnNiAl-LDH precursor calcined at 500 °C show the highest photocatalytic activity, the maximum yield of 2680 umol·$gcat^{-1}$ methanol within 6 h was obtained with 0.04 mol of NaOH and Na_2SO_3, respectively. The mechanism of CO_2 photocatalytic reduction over ZnO/NiO/$ZnAl_2O_4$ was discussed.

Kaouther *et al.* (2017) reported that [Zn-Al] layered double hydroxides (LDH) with cationic molar ratios of R = Zn/Al 1:5 were synthesized by the coprecipitation method at constant pH = 10. The samples synthesized and their derived forms obtained after calcination at 500°C and at 900°C (denoted Zn-Al-R, Zn-Al-R-500 and Zn-Al-R-900, respectively), were

characterized by X-ray diffraction (XRD), inductively coupled plasmamass spectrometry, scanning electron microscopy, energy-dispersive X-ray spectroscopy, diffuse reflectance spectroscopy and nitrogen physisorption at –196°C. The XRD study showed the presence of accessory ZnO with the LDH in samples synthesized with $R \geq 3$; and the lamellar structure was destroyed at 500°C which made room for a poorly ordered ZnO phase, while calcination at 900°C yielded well crystallized ZnO and $ZnAl_2O_4$. The photocatalytic activity of the calcined and the unheated samples was evaluated for the decolourization of methylene blue. The photocatalytic activity was dependent on the cationic ratio R and on the calcination temperature. The sample Zn-Al displayed maximum photocatalytic activity. Calcination at 500 and 900°C improved the photocatalytic activity of LDH synthesized at R = 1 and 2.

Zhe-Ming *et al*. (2017) investigated a series of Zn/M–NO_3-LDHs (M = Al, Fe, Ti, and Fe/Ti) have been synthesized by two different methods, and their activities for visible-light photocatalytic degradation on Rhodamine B (RB) were tested. Solids were analyzed by XRD, FT-IR, and ICP characterization, confirming the formation of pure LDH phase with good crystal structure. It was observed that the band gap of these nitrate LDH materials was following this order: Zn/Fe–NO_3-LDHs (2.55 eV) > Zn/Fe/Ti–NO_3-LDHs (2.88 eV) > Zn/Ti–NO_3-LDHs (3.03 eV) > Zn/Al–NO3-LDHs (3.23 eV); however, the degradation performance of RB by four materials followed the order: Zn/Ti–NO3-LDHs (98%) > Zn/Al–NO_3-LDHs (96%) > Zn/Fe/Ti–NO_3-LDHs (88%) > Zn/Fe–NO_3-LDHs (72%). In addition, a possible mechanism for photocatalytic degradation on RB has also been presumed. Moreover, after three regeneration cycles, the percentage of RB degradation rate was still close to 90%.

Amor *et al*. (2018) reported the synthesis of Zn-Al-Ti layered double hydroxides (LDHs) powders with coprecipitation. The characteristics of the samples were investigated X-ray

diffraction (XRD), scanning electron microscopy (SEM) and spectrophotometer UV–Vis (DRS). Non-uniform distribution was shown for LDHs samples by SEM. Photocatalytic efficiencies were tested using methylene blue (MB) dye as a model contaminant under UV irradiation. In particular, Zn–Al-Ti LDH exhibited an excellent performance towards MB degradation compared with commercial TiO_2 nanoparticles. Methylene blue removal percentage was reached at almost 100%, whereas commercial TiO_2 reached a removal rate of only 66% under the same conditions within 20 min.

Martinez *et al*. (2018) reported that MgAl layered double hydroxides (LDHs) materials are the most representative materials of the hydrotalcite compounds, which exhibit a high CO_2 adsorption at room temperature. The MgAl LDHs materials were synthesized by microwave-hydrothermal method to obtain photocatalysts with high efficiencies for solar fuels generation from CO_2 photoconversion in liquid and gas phases. During the synthesis of MgAl LDHs, the effect of Mg^{2+} precursor and the microwave irradiation time on the physical and chemical properties developed by the materials were evaluated. Some differences among the MgAl LDHs obtained were found by means of XRD, UV–vis reflectance diffuse, FTIR, and potentiodynamic electrochemical impedance spectroscopy. The results demonstrated that the MgAl materials had a higher selectivity for generation of products in liquid phase such as CH_3OH probably because of the potential value of their conduction band and the thermodynamic limitations for CH_4 production. The evaluation of the materials synthesized in photocatalytic CO_2 conversion showed an increase in the methanol production by increasing microwaves irradiation time and employing an organic precursor as Mg^{2+} source. The photocatalytic activity was favored in the MgAl LDH materials with high crystallinity and with a more negative flat band potential to carry out the CO_2 reduction.

CHAPTER THREE

MATERIALS AND METHODS

3.1 Materials

Glassware, Equipment and Instruments are the material are the material used in this research work

3.1.1 Apparatus

The apparatus used are shown in the table 3.1 below

Table 3.1: Lists of Apparatus

S/N	Apparatus	Capacity/Model
1	Conical flasks	250ml
2	Magnetic stirrer	
3	Thermometer	
4	Volumetric flasks	100ml,250ml, 1000ml
5	Beakers	100ml,250ml,500ml,1000ml

3.1.2 Instruments

The Instruments used are listed in the table below:

Table 3.2: List of Instruments

S/N	Instruments	Model/Company
1	Fourier transform infrared spectroscopy	Cary 630; Agilent Technologies
2	Scanning Electron Microscope	Leica Stereo, Scan-440
3	X-ray Diffraction Machine	Oxford Instruments
4	pH Meter	3510 Jenway
5	Weighing balance	FA2004
6	UV-Vis spectrophotometer	Cary 50; Version 3.0
7	Centrifuge Machine	24D Spectrafuge

3.1.3 Chemicals

All chemicals used in this research work were of analytical grade.

Table 3.3: List of Chemicals

S/N	Chemicals	Purity	Manufacturer
1	Phosphoric acid	99%	Sigma
2	Cadnium flouride		Sigma
3	Aluminium chloride		Sigma
4	Antimony chloride		Sigma
5	Hydrochloric acid	97%	Sigma

3.2 METHODS

PREPARATION OF REAGENTS

3.2.1 Preparation of 0.1M NaOH

0.4g of NaOH was dissolved in a small amount of distilled water in a beaker. The solution was then transferred into a 100 ml volumetric flask and made to the mark with distilled water and labeled as 0.1M NaOH.

3.2.2. Preparation of 0.1M HCl

8.35cm^3 of the concentrated HCl was measured using measuring cylinder and transfer in to a beaker containing some distilled water, the content was transfer in to 100 ml volumetric flask and made to the mark with distilled water and labelled as 0.1M HCl.

3.2.3 Preparation of the Dyes Stock and Working Solution

Stock solution (1000 ppm) of RB and M.R. was prepared by dissolving separately 1.0g of each dye in a beaker containing small amount of distilled water until homogenous solution was obtained. The resulting solution was quantitatively transferred into 1000 cm^3 volumetric flasks and diluted to the mark. Intermediate stock of 100 ppm was prepared from the stock by appropriate dilution. Four different concentrations (3 ppm, 6 ppm, 9 ppm and 12 ppm) were prepared from intermediate stock using the same dilution formula and used as working solutions.

3.3 Preparation of Activated Carbon From Rice Husk

The Rice Husk was acquired from Dawanau market of Kano state on 4/04/2017. The rice husk was washed thoroughly with warm water to remove sand and some water soluble substances. The rice husk was dried in an oven at temperature of 100^oC for 4 h.

20g of the rice husk was added to 200cm^3 of 10% (V/V) H_3PO_4 (Molina and Rodrigues, 2004). Rice husk was washed several times until neutral pH was obtained in both litmus paper and pH indicator. After washing, the sample was dried in an oven for 8hours at temperature of 100^oC, the dried sample was then carbonized in a muffle furnace at a temperature of 450^oC for one hour. The activated carbon was cooled inside the furnace. The AC allowed pass 1mm size mesh to remove those with larger sizes. The carbon was stored in a moisture free container prior to further use.

3.4 Synthesis of Cd-Al/AC-LDH.

Salts of Cadmium fluoride (CdF_2) and Aluminium chloride ($AlCl_3$) were well mixed in distilled water and then mixed with activated carbon through co-precipitation method (Khan *et al*., 2016). 200.25g of $AlCl_3$ salt and 84.5g of CdF_2 were dissolved in distilled water. To this reaction mixture, 1g of activated carbon was added and well dispersed by continuous stirring with the help of magnetic stirrer. To this mixture freshly prepared 0.1 M NaOH solutions was added and continuously monitored till pH 9. After this, the reaction mixture was placed on a hot plate for 6 h at 60 °C with homogenous stirring. After completion of the reaction the surplus solution is removed and the precipitate was washed three times with C_2H_5OH:H_2O mixture (8:2). The derived product was dried in an oven for overnight at 50 °C and store in clean tube for further characterization.

3.5 Synthesis of Cd-Sb/AC-LDH.

Salt of Cadmium fluoride (CdF_2) and Antimony chloride ($SbCl_3$) were well mixed in distilled water and then mixed with activated carbon through co-precipitation method (Khan *et al*., 2016). 342.75g of $SbCl_3$ salt and 84.5g of CdF_2 were dissolved thoroughly in distilled water. To this reaction mixture, 1g of activated carbon was added and well dispersed by continuous stirring with the help of magnetic stirrer. To this mixture freshly prepared 0.1 M NaOH solutions are added and continuously monitored till pH 9. After this, the reaction mixture was placed on a hot plate for 6 h at 60 °C with homogenous stirring. After completion of the reaction the surplus solution is removed and the precipitate was washed three times with C_2H_5OH:H_2O mixture (8:2). The derived product was dried in an oven for overnight at 50 °C and store in clean tube for further characterization.

3.6 CHARACTERIZATION OF LDHs

Both catalysts Cd-Sb/AC and Cd-Al/AC LDHs were characterized using X-ray Diffaraction (XRD), Scanning electron Microscopy (SEM) and Fourier Transform Infrared Spectroscopy (FT-IR).

3.6.1 X-ray diffraction (XRD) analysis

The crystallographic structure of the LDHs were achieved by X-ray diffraction (XRD) analysis. This is done by irradiating the catalysts of the LDHs with incident X-rays and then measuring the intensities and scattering angle of X-ray that are scattered by Cd-Al/AC and Cd-Sb/AC layered double hydroxide catalysts.

3.6.2 Determination of Crystallite Size

The crystallite size of the sensitized catalysts was calculated using Debye Scherer and Williamson Hall methods. The XRD data was analyzed using Full Proof Suite 3.0.

Debye Scherer Method

The particle size was calculated using Debye-Scherer's equation as shown in equation 9.

$$D = \frac{K\lambda}{\beta cos\theta} \quad \text{.....(9)}$$

Where D is the crystallite size in nanometer, K is a constant whose value is approximately 0.9, λ is the wavelength of X-ray Radiation source (CuKα 0.1546nm), β is the full width at half maximum intensity (FWHM) in radians, θ is Bragg angle at the position of peak MaximumThe d-spacing between planes is in atomic lattice was calculated using Bragg equation (Equation 10)

$2dsin\theta = n\lambda$……..……(10)

The values of β where determine using the application WINPLOTR, which comes in with the Full proof 3.0 XRD software package.

3.7 Scanning Electron Microscopy (SEM) Analysis

The surface morphology of the LDHs were achieved by using Scanning electron microscopic (SEM) analysis. SEM is test processes that scan Cd-Al/AC and Cd-Sb/C LDH catalysts with an electron beam to produce a magnified image for analysis.

3.8 Fourier Transform Infra-Red (FTIR) Analysis.

Qualitative analyses of the main functional groups that are present in the LDHs were determined with a FT-IR spectrophotometer. FTIR-Cary 630 from Agilent technologies was used and the spectra were recorded in the wavelength interval 4000 to 750 cm^{-1}. Four (4) scans is enough because the peaks will stand out, no matter how much baseline noise there is. The FT-IR analysis method uses infrared light to scan Cd-Al/AC and Cd-Sb/AC LDH catalysts and observed chemical property.

3.9 Determination of Band Gap Energy

The band gap energies of both synthesize catalysts were determine using the Tauc Plot Method. The following procedure was used to determine the band gap.

1. The absorbance of samples Cd-Al/AC and Cd-Sb/AC were measured using Perkin Elmer Lambda 35 UV/Vis/NIR spectrophotometer
2. The relation expression proposed by Tauc, Davis and Mott was used

$$(h\nu\alpha)^{\frac{1}{n}} = A(h\nu - E_g) \quad \text{.....(11)}$$

Where: h: Plank's constant=6.623×10^{-34}Js, v: frequency of vibration, α: absorption coefficient, E_g: band gap, A proportional constant. Since the direct allowed sample transition is used in this expirement, the value of the denominator of the exponent was set n=1/2

3. A line is drawn tangent to the point of intersection of the tangent line and the horizontal is the band gap Eg value.

3.10 Photocatalytic Experiment

In a typical experiment, 100mg of either Cd-Al/AC or Cd-Sb/AC was dispersed in 100cm^3 of each dye solution having a concentration 3ppm (RB or M.R.) in a beaker. The above suspension was magnetically stirred for 25 mins in the dark to obtained adsorption-desorption equilibrium to eliminate the error due to any initial adsorption effect. This was then irradiated using 500W high-pressure Hg lamp of intensity 0.0129w/m^2. A 5cm^3 aliquot was taken at 25 mins interval, centrifuged at 2000rpm prior to absorbance measurement in order to eliminate error due to scattering (Li *et al.,* 2008).

The catalytic activities of Cd-Al/AC-LDH and Cd-Sb/AC were evaluated against the respective dyes under visible light. The effect of operational parameters such as time, catalyst dosage, pH and concentration were investigated, the percentage removal efficiency R.E. (%) of each catalyst was evaluated by using the following equation.

$$\text{R.E.}(\%) = \left(\frac{Co-Ct}{Co}\right) \times 100 = \left(\frac{Ao-At}{Ao}\right) \times 100 \quad \ldots\ldots(12)$$

C_0 represents the original concentration of each dye solution at time = 0, Ct is the concentration of dye solution by adding the catalyst after some time = t as indicated in equation. Similarly, A_0 designated the absorbance of the original concentration of the dye solution at time = 0 and At is the absorbance of dye solution during reaction progress after passing some time = t (Li *et al.*, 2008).

3.10.1 Effect of Catalyst Dosage on Photodegradation of RB and M.R.

The amount of catalyst powder may also affect the process of dye degradation. The effect of catalyst dosage was monitored by separately contacting 200 cm^3 of each dye (3ppm), with 50mg, 100mg, 150mg and 200mg, of either Cd-Al/AC or Cd-Sb/AC in a beaker under visible light irradiation. The mixture was magnetically stirred for 100 mins. A 5cm^3 of sample was taken and centrifuged at 2000 rpm. The absorbance of the sample was measured at 554nm for RB using UV-visible Spectrophometer while for M.R. the absorbance of the sample was measured at 463nm.

3.10.2 Effect of pH on Photodegradation of RB and M.R.

The pH of the reaction medium has a significant effect on the surface properties of Cd-Al/C and Cd-Sb/C catalyst. The effect of pH was investigated by separately combining 200cm^3 of each dye (3ppm) with 200mg of either Cd-Al/AC or Cd-Sb/AC, at pH 5, pH 7, pH 9 or pH 12 in a beaker under visible light irradiation. The mixture was magnetically stirred for 100 mints. A 5cm^3 aliquot was taken and centrifuged at 2000rpm. The absorbance of the sample was measured at

554nm for RB using UV-visible Spectrophometer while for M.R. the absorbance of the sample was measured at 463nm.

3.10.3 Effect of Concentration of Dye on Photodegradation of R.B. and M.R.

The effects of dye concentration on the degradation of Rhodamine B and Methyl red were studied by separately contacting 200cm^3 of 3ppm, 6ppm 9ppm and 12ppm of RB or MR, at pH 12 for RB and pH 5 for M.R., with 200mg of each catalyst (Cd-Al/AC or Cd-Sb/AC), in a beaker under visible light irradiation. The mixture was magnetically stirred for 100 mins. A 5cm^3 aliquot was taken and centrifuged at 2000rpm. The absorbance of the sample was measured at 554nm for RB using UV-visible Spectrophometer while for M.R. the absorbance of the sample was measured at 463nm.

CHAPTER FOUR

4.0 RESULTS AND DISCUSSION

4.1RESULTS

4.1.1 Characterization of Cd-Al/AC and Cd-Sb/AC LDHs

Both catalysts Cd-Sb/AC and Cd-Al/AC LDHs were characterized using X-ray Diffaraction (XRD), Scanning electron Microscopy (SEM) and Fourier Transform Infrared Spectroscopy (FT-IR).

a. X-ray Diffaraction (XRD) of Cd-Al/AC and Cd-Sb/AC LDHs

The crystalline phases of the prepared samples were characterized by XRD analysis. The XRD patterns of Cd-Sb/AC and Cd-Al/AC are shown in Figures 4.1a and 4.1b respectively. The characteristic peaks for Cd-Sb/AC-LDH appeared at 2θ = 10.0 (003) which was not found in Cd-Al/AC. The 2θ = 23.4 (006) and 2θ = 35.5 (012) suggesting the formation of Cd-Al/C-LDH.

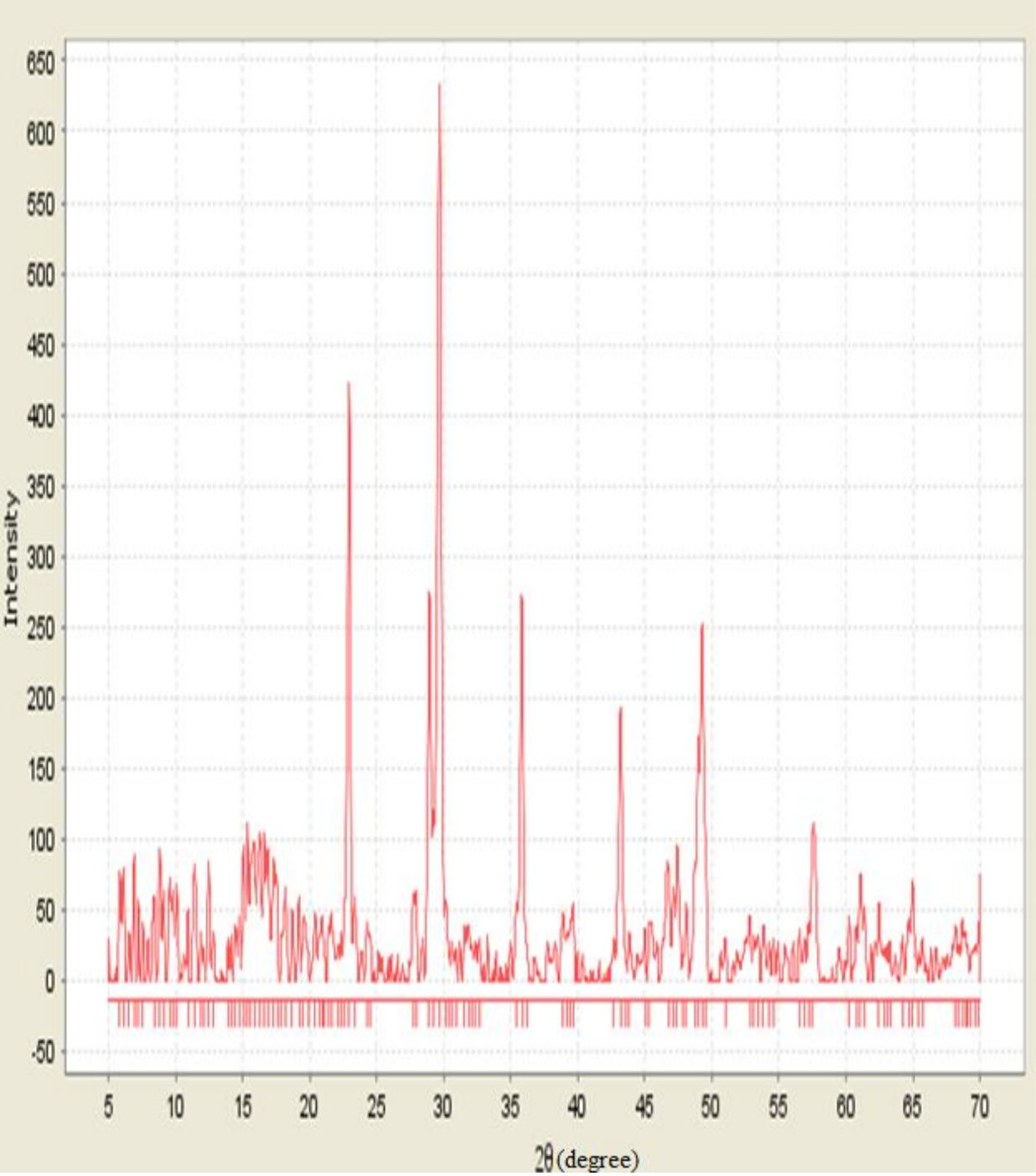

Figure 4.1a: XRD of patterns of the Cd-Al/AC LDH catalysts.

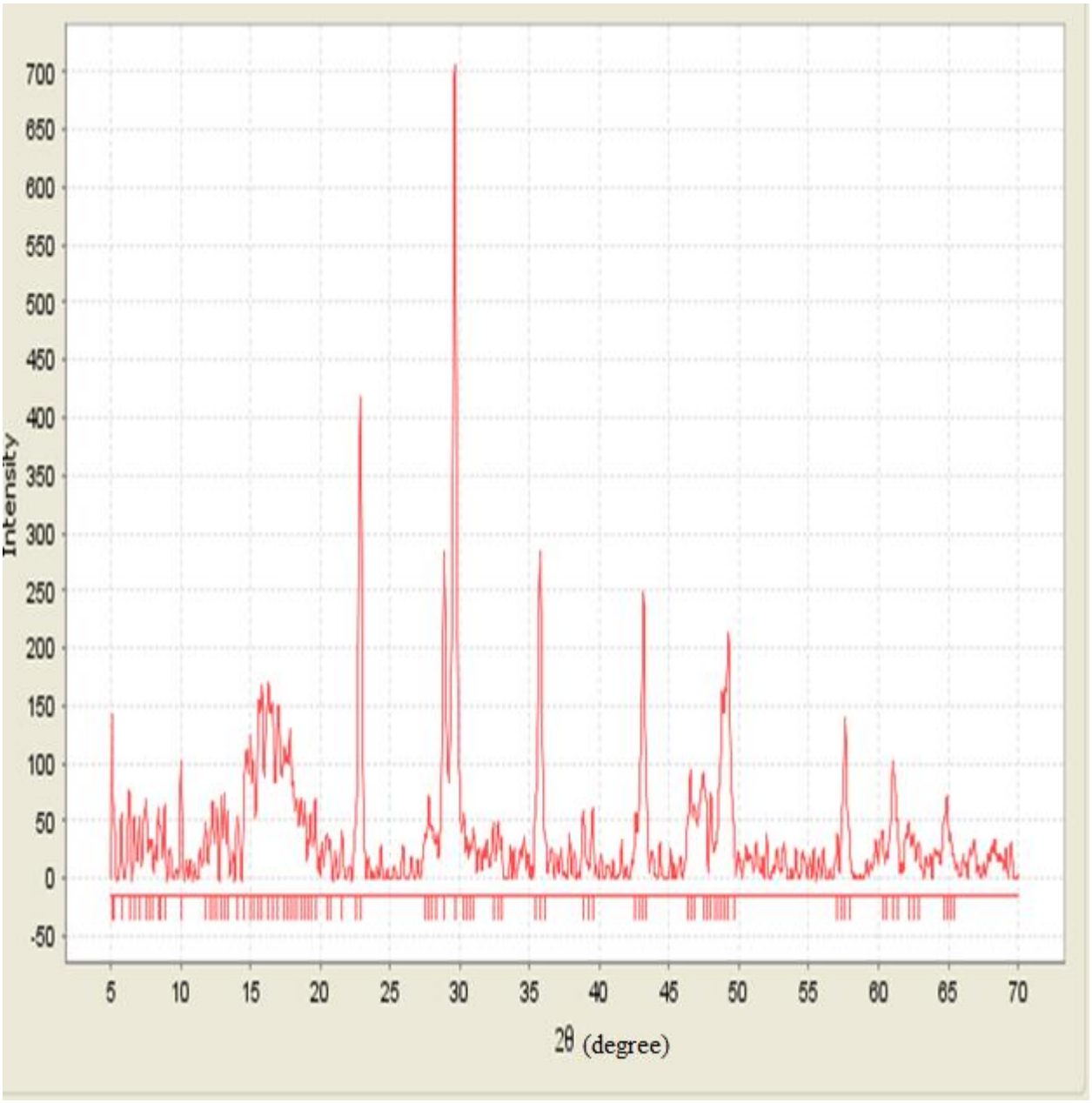

Figure 4.1b: XRD pattern of the Cd-Sb/C LDH catalyst

b. Scanning Electron Microscopy (SEM) of Cd-Al/AC and Cd-Sb/AC LDHs

Scanning Electron Microscopy gave further insights into the morphology and size details of the Cd-Al/AC and Cd-Sb/AC LDHs. The surfaces morphology of Cd-Al/AC and Cd-Sb/AC LDHs are shown in Figures 4.2 and 4.3. The SEM images showed that the sheet morphology of Cd-Al/AC and Cd-Sb/AC, which indicated that the agglomerated grains are not uniform.

Figure 4.2 SEM image of the Cd-Al/AC LDH catalyst.

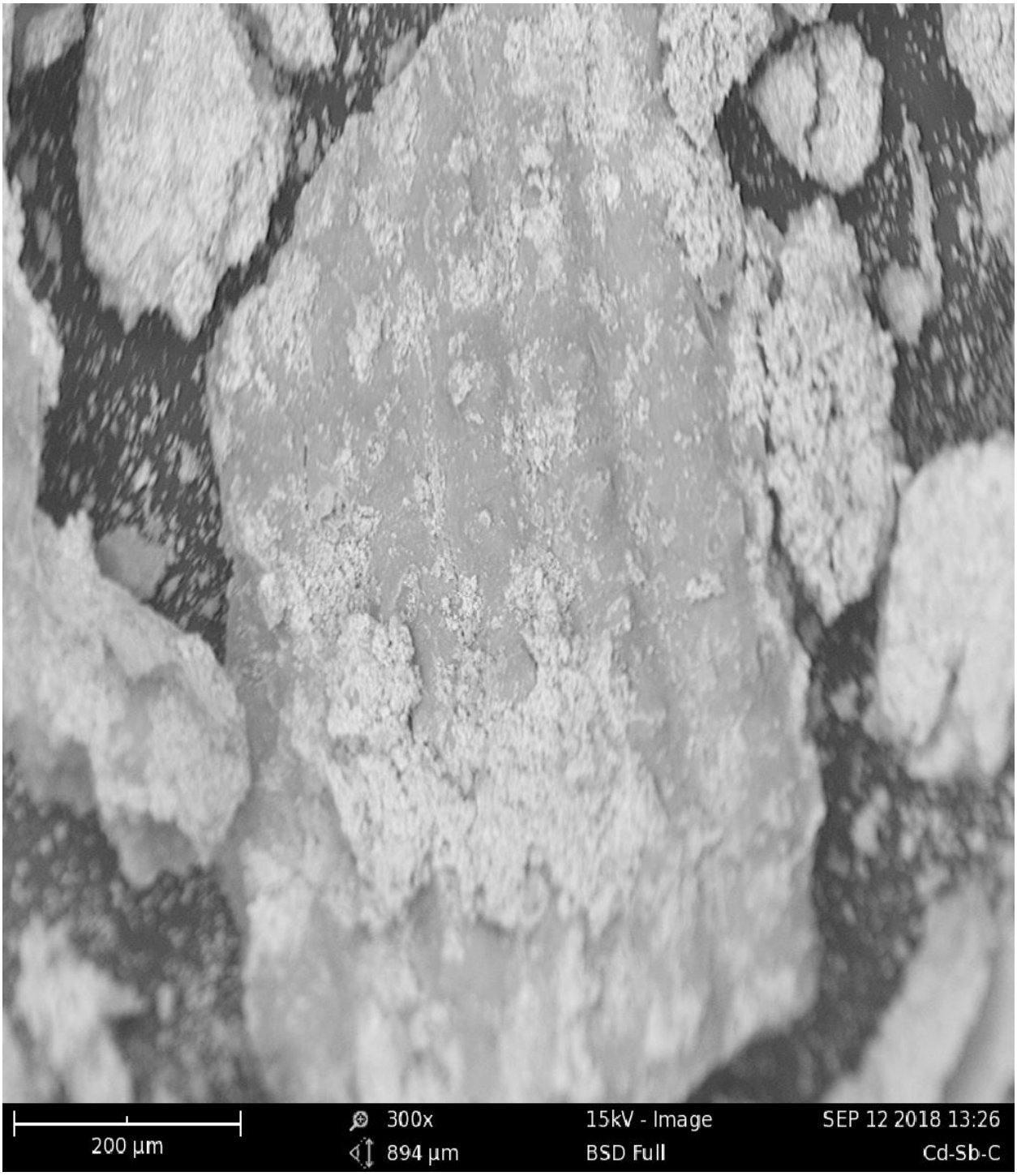

Figure 4.3 SEM image of the Cd-Sb/AC LDH catalyst.

c. **Fourier Transform Infrared Spectroscopy (FT-IR) of the Cd-Al/AC and Cd-Sb/AC LDHs**

FT-IR spectroscopy was used to determine the main functional groups responsible for Cd-Al/AC and Cd-Sb/AC LDHs formation and other important available functional groups. The FTIR spectra of the prepared Cd –Al/AC and Cd-Sb/AC LDHs are shown in Figures 4.4 and 4.5. The spectra showed a broad absorption band at 3387.58 cm^{-1} and 3379.5 cm^{-1} which is referred to O-H stretching mode of the hydroxyl group in the layers of Cd-Al/AC and Cd-Sb/AC LDHs, respectively

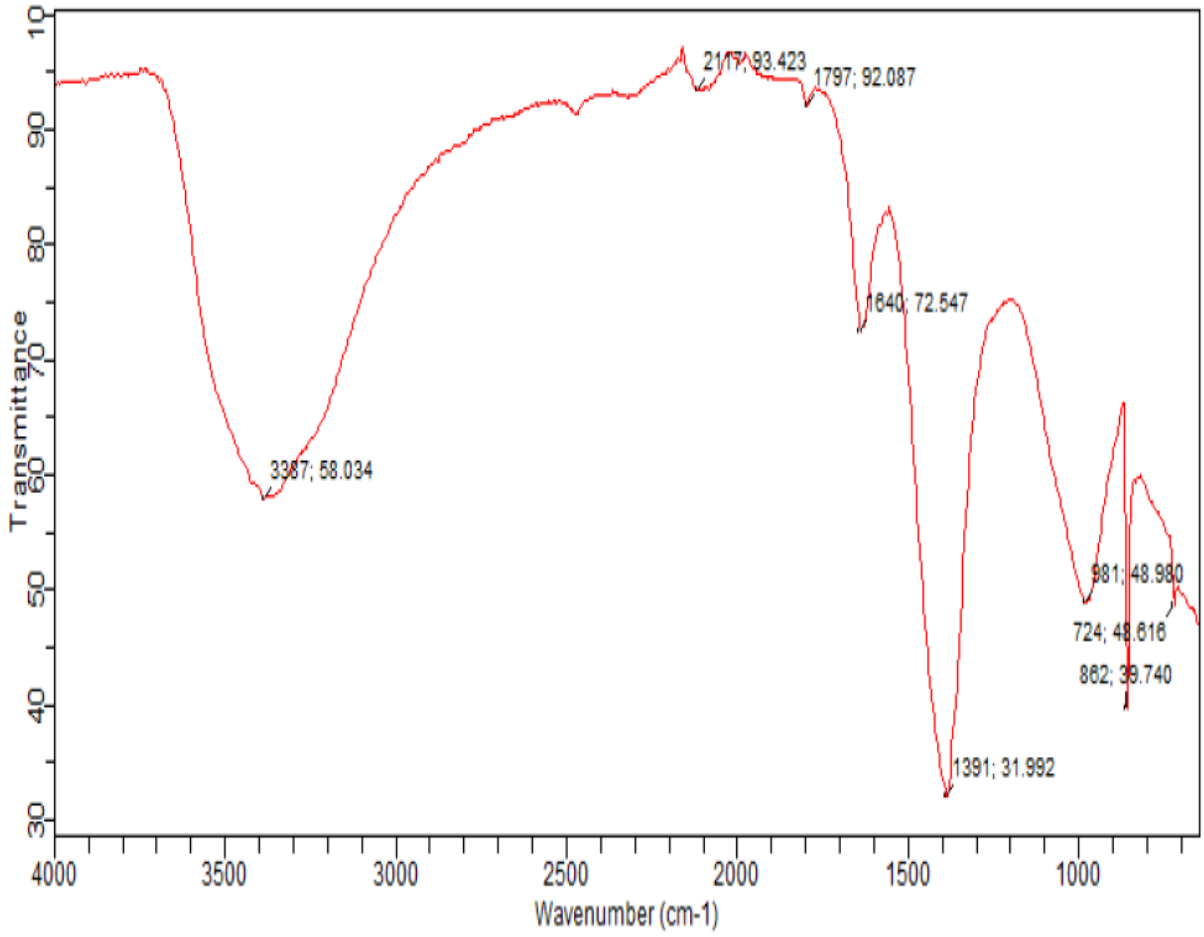

Figure 4.4: FT-IR Spectra of the Cd-Al/AC LDH catalyst.

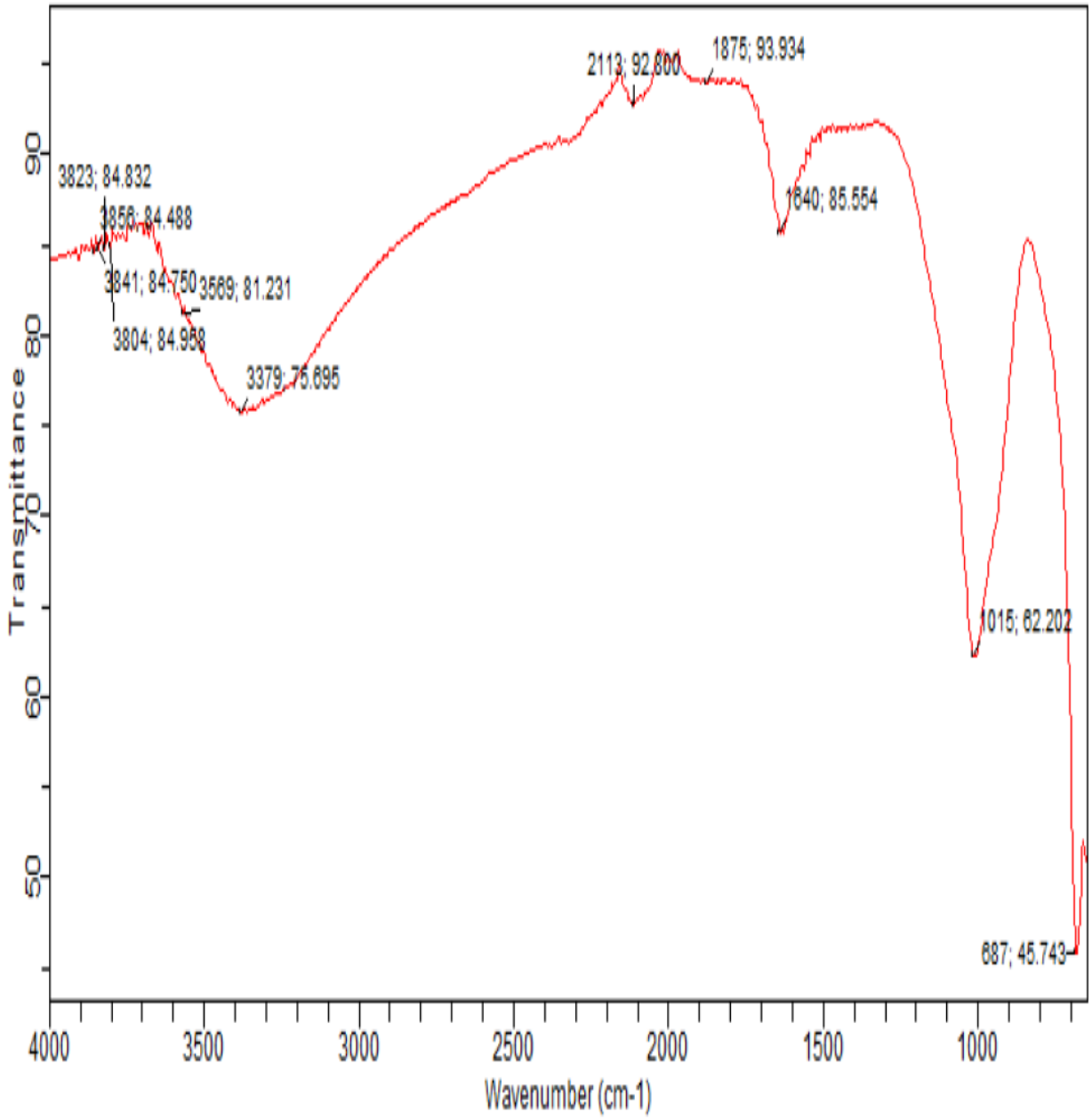

Figure 4.5: FT-IR Spectra of the Cd-Sb/AC LDH catalyst.

d. Band Gap Energy

The UV–visible absorption spectra of Cd-Al/C and Cd-Sb/C are depicted in Figures 4.6 and 4.7.

The *Eg* values were also estimated based on the Tauc equation.

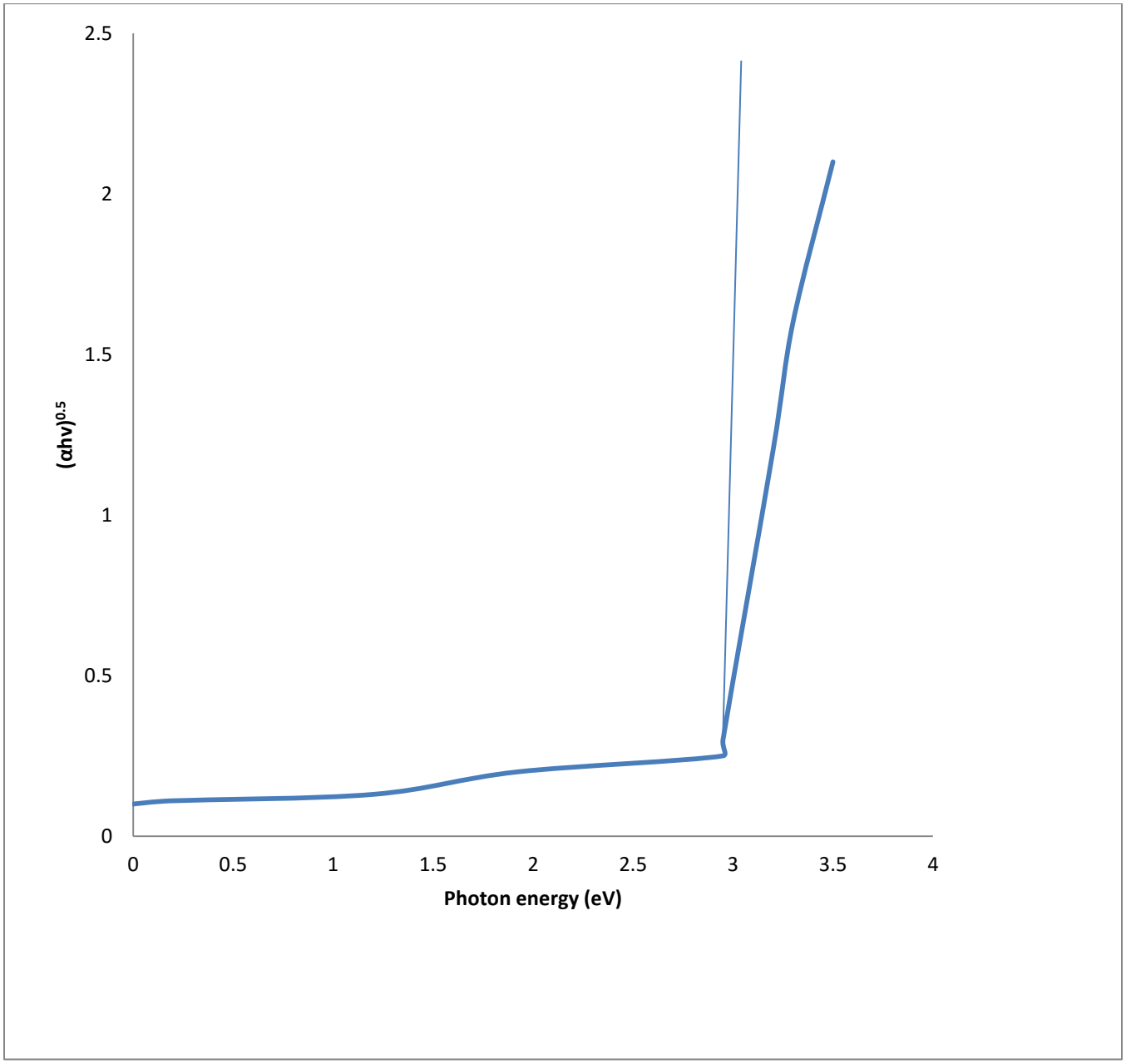

Figure 4.6: The Tauc plot showing the energy band gap of Cd-Al/AC LDH catalyst.

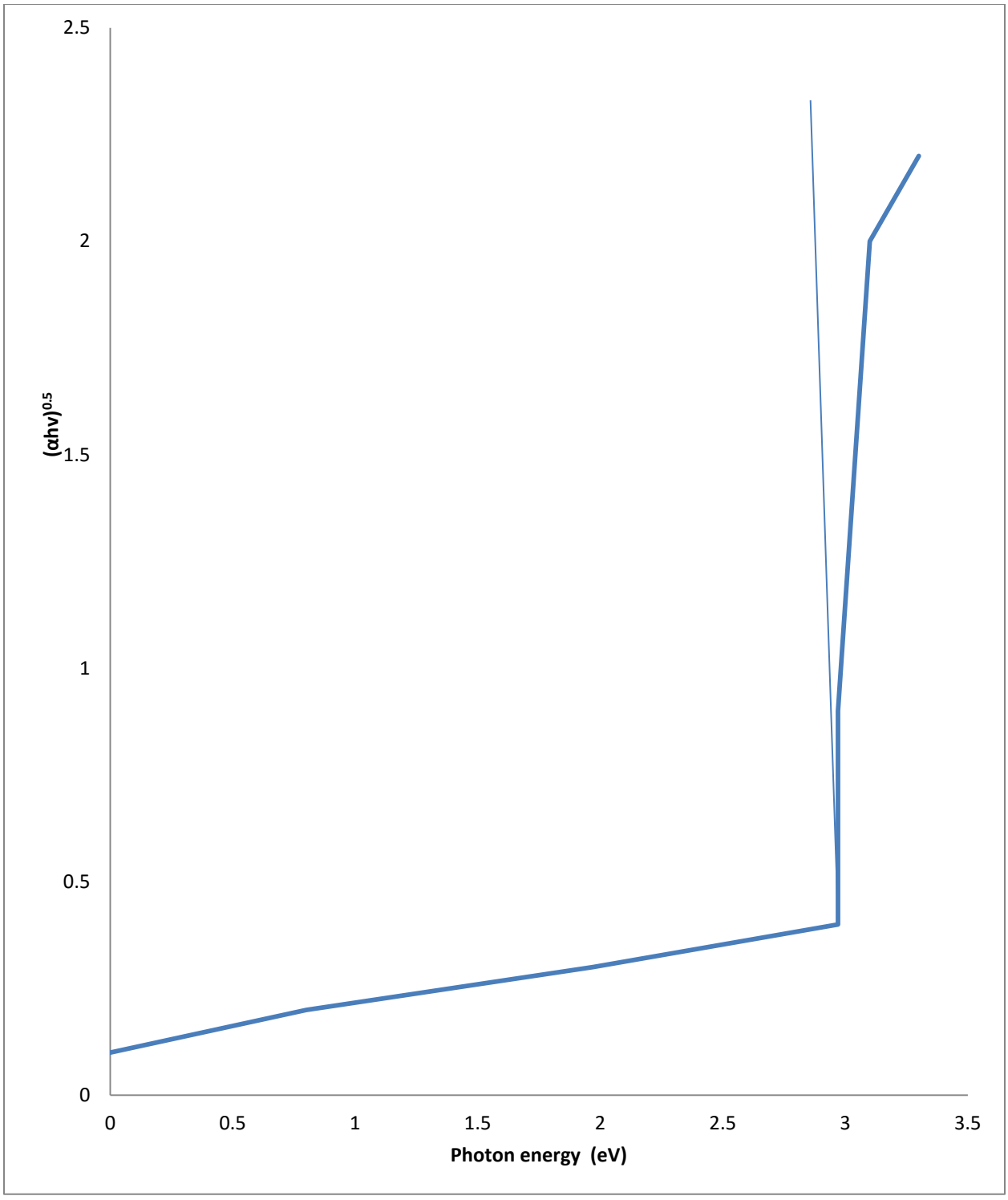

Figure 4.7: The Tauc plot showing the energy band gap of Cd-Sb/AC LDH catalyst.

4.1.2 Effect of Operational Parameters

The effect of operational parameters such as catalyst dosage, pH and initial dye concentration were tested using Cd-Sb/AC and Cd-Al/AC LDHs on degradation of Mehyl Red and Rhodamine B dyes.

a. Effect of Catalyst Dosage

Dye degradation is also affected by the amount of the photocatalyst used. The dye degradation increases with increasing catalyst concentration, which is characteristic of heterogeneous photocatalysis. The increase in catalyst amount actually increases the number of active sites on the photocatalyst surface thus causing an increase in the number of $^{\bullet}OH$ radicals which can take part in actual discoloration of dye solution. (Shankar *et al*., 2004).

The effect of catalyst dosage is as shown in Figure 4.8.

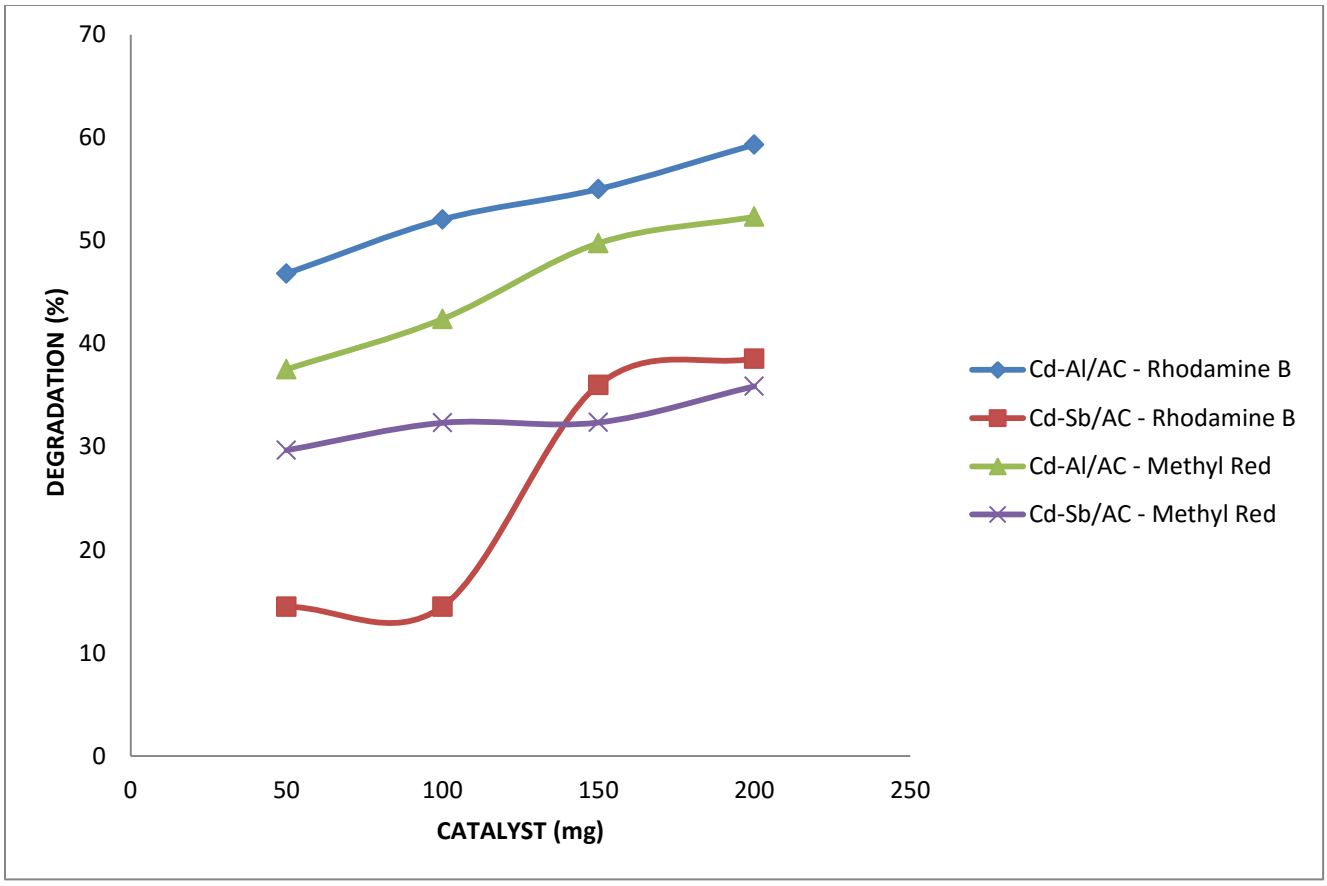

Figure: 4.8 Effect of catalyst dosage on the degradation of RB and MR using Cd-Al/AC and Cd-Sb/AC LDHs catalysts

b. Effect of pH

The pH value of the aqueous solution is a key parameter for photocatalytic degradation of wastewater and dyes because it affects the adsorption of pollutants that happens at the surface of Photocatalysts (Zielinska *et al.*, 2007).

The effects of pH is as shown in Figure 4.9

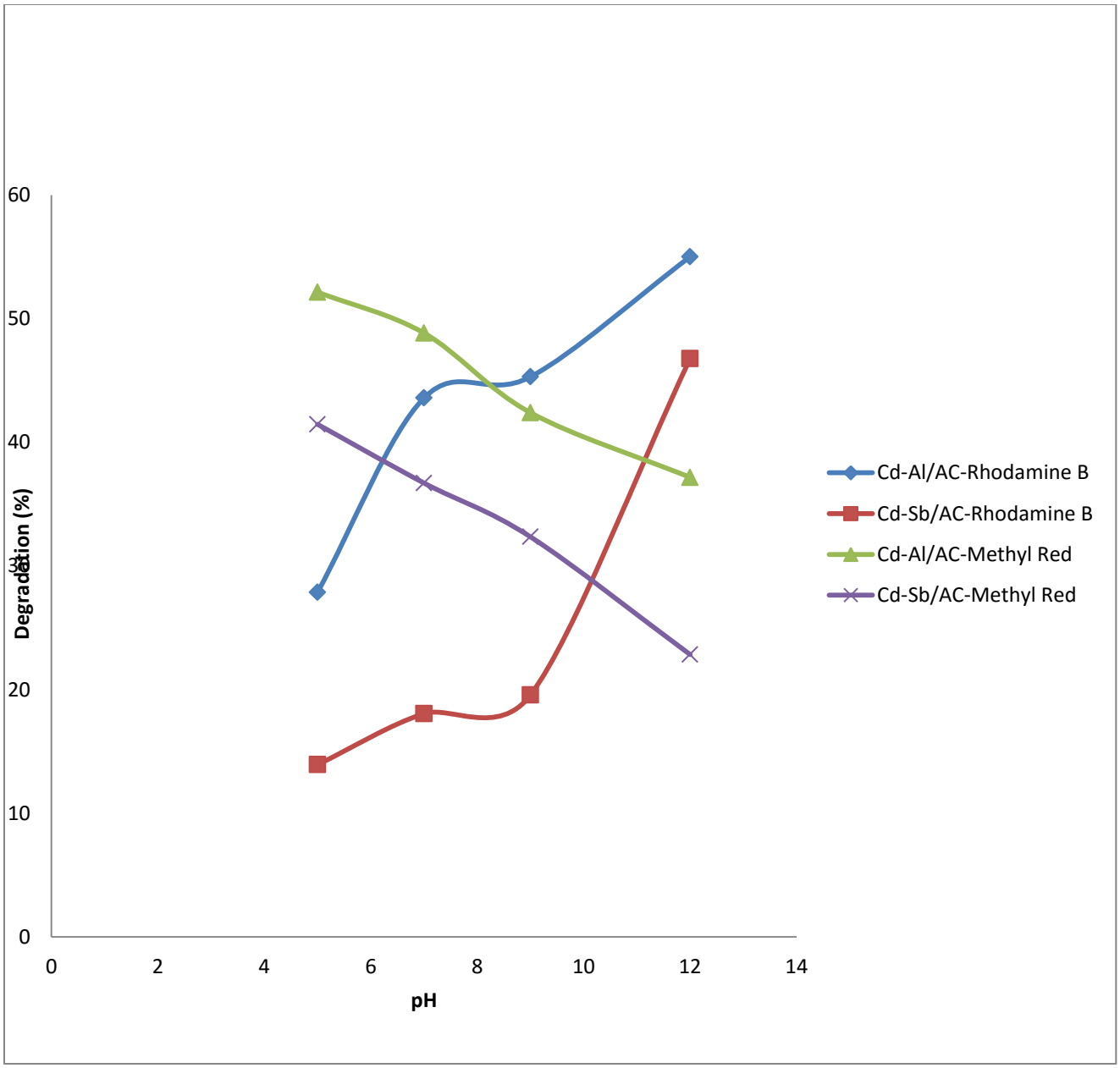

Figure: 4.9 Effect of pH on the degradation of RB and M.R. using Cd-Al/AC and Cd-Sb/AC LDHs

c. Effect of Concentration

The initial concentration of dye in a given photocatalytic reaction is also another aspect which needs to be taken into account. It is generally found that percentage degradation decreases with increasing amount of dye concentration, while keeping a fixed amount of catalyst (Macedo *et al*., 2007).

The effects of concentration are shown in Figure 10.

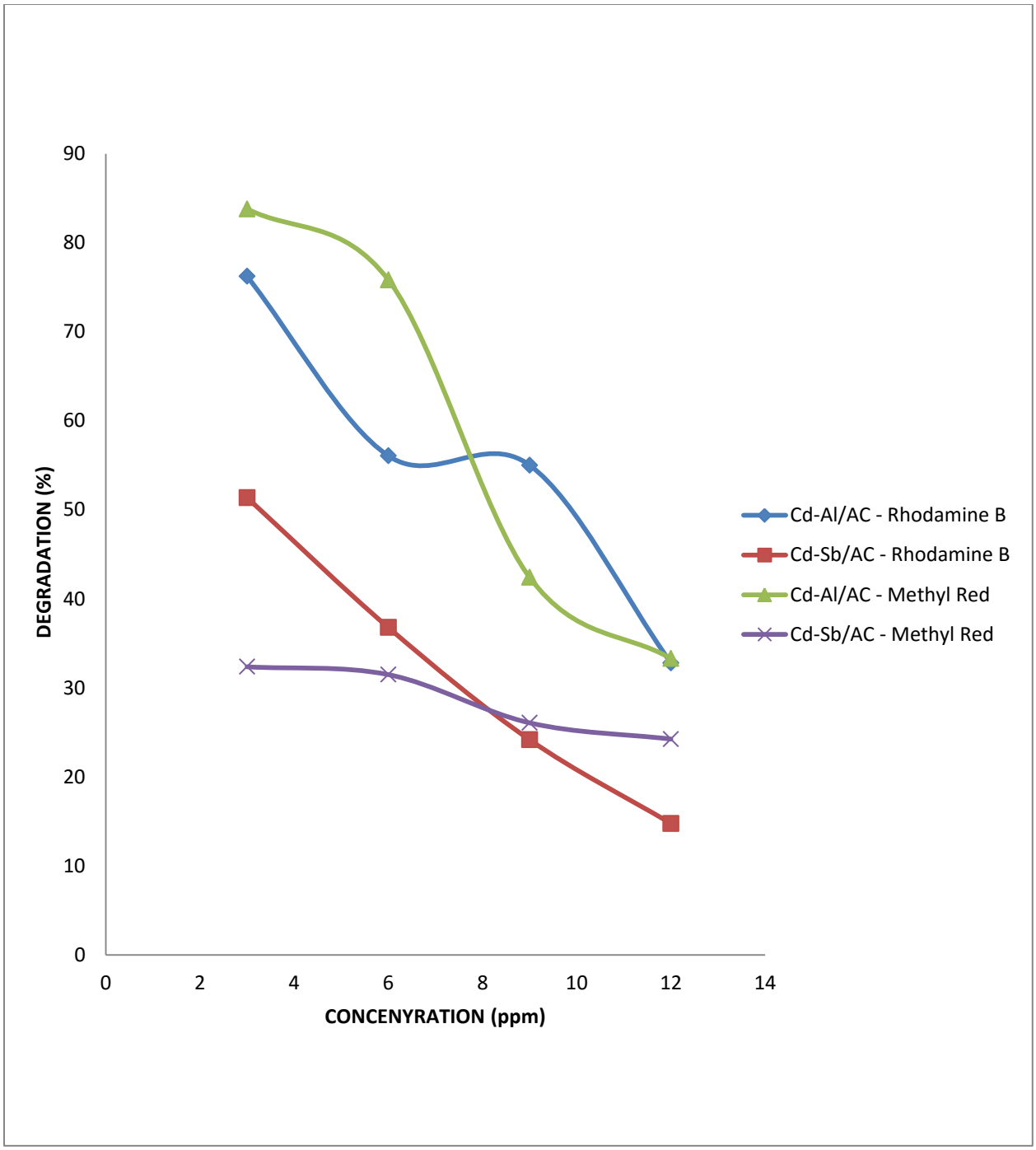

Figure 4.10: Effect of dye concentration on the degradation of R.B and M.R. using Cd-Al/AC and Cd-Sb/AC LDHs.

d. KINETIC STUDIES

Kinetic studies were employed in order to carefully monitor and intreprete the kinetic of photocalytic process involving two catalysts. The kinetic of the dyes were analysed by pseudo first order and pseudo second order. The results are summarized and presented in Table 4.1

Table 4.1: Kinetic Models and Calculated Parameters on Photodegradation of Rhodamine B and Methyl Red using Cd-Sb/C and Cd-Al/C.

DYES	CATALYST	Pseudo First Order		Pseudo Second Order	
		K	R^2	K	R^2
Rhodamine B	1) Cd-Sb/C	0.026	0.9556	0.02850	0.9863
	2) Cd-Al/C	0.0209	0.890	0.04778	0.996
Methyl Red	1) Cd-Sb/C	0.007	0.853	0.0089	0.9702
	2) Cd-Al/C	0.0225	0.9958	0.045	0.9778

4.2 DISCUSSION

4.2.1 Catalyst Characterization

a. X-ray Diffraction (XRD)

The crystalline phases of the Synthesized Cd-Al/AC and Cd-Sb/AC LDHs were characterized by XRD analysis. Figures 4.1a and 4.1b displayed the XRD patterns of the prepared Cd-Al/AC and Cd-Sb/AC LDHs, respectively. The characteristic peaks for Cd-Sb/AC-LDH appeared at 2θ = 10.0 (003) which was not found in Cd-Al/AC. The 2θ = 23.4 (006) and 2θ = 35.5 (012) suggesting the formation of Cd-Al/C-LDH. The 003 and 006 corresponding to the basal reflection of the successive stacking of brucite like layers (El Gaini *et al*., 2009). The strong diffraction peaks at low angle due to basal planes (003), (006), were sharp and symmetric compared to the peaks at high angle, which are characteristic of clay minerals having a layered structure (parida *et al* 2006). From Figures 4.1a and 4.1b, one can observe strong signals in the 2θ range of 2-30^{o}. These peaks indicated that the prepared LDHs are characterized by low crystalinity and consistent to great extent, with the peaks of hydrotalcite structure (Ren *et al*., 2007).

Powder X-rays diffraction (XRD) patterns were recorded with a Thermo scientific XRD machine of model ARL X" TRA with X-ray diffractometer. The intensities were obtained in the 2θ ranges between 20° and 70°. The FULPROF software was used for data handling. FULPROF software allowed estimating the average size of the crystallites. Refinement was performed on the diffraction patterns to determine the crystallite size and relative abundance of phases.

The D values are 101 and 128 nm for Cd-Al/AC and Cd-Sb/AC respectively.

b. Scanning Electrode Microscopy (SEM)

Figures 4.2 and 4.3 show the comparison of SEM images for Cd-Al/AC and Cd-Sb/AC LDHs catalysts. The SEM images showed that the sheet morphology of Cd-Al/AC and Cd-Sb/AC, which indicated that the agglomerated grains are not uniform. The agglomerated pattern is evidence in the formation of LDHs and the morphology of the LDHs are in line with report for LDHs (Hibino and Kobayashi, 2005). However, the particles are clearer in Cd-Al/AC than Cd-Sb/AC (Yudong *et al*., 2014).

c. FT-IR (Fourier Transform Infrared Spectroscopy)

The FTIR spectra of the Synthesized Cd –Al/AC and Cd-Sb/AC LDHs are represented in Figures 4.4 and 4.5 respectively. The spectra showed a broad absorption band at 3387.58 cm^{-1} and 3379.5 cm^{-1}which is referred to O-H stretching mode of the hydroxyl group in the layers, of Cd-Al/AC and Cd-Sb/AC LDHs, respectively. These bands are commonly observed in the LDHs materials (Cavani *et al*., 1991). At about 1391 cm^{-1} there is a characteristic signal of COO^- stretching which is presence in Cd-Al/AC. Gasser and Aly (2009) reported the bands at 1394 cm^{-1} attributed to the vibration of COO^-. The absorption peaks in the low frequency region, for M-O is below 862cm^{-1} and 687cm^{-1}in the Cd-Al/AC and Cd-Sb/AC LDHs, respectively (Tanaka *et al* ., 2010).

Table 4.2: Fourier Transform Infra-Red Spectroscopic Data

Catalysts	Bond Stretching	Spectral Value cm^{-1}
Cd-Al/C	O-H	3387
	COO^-	1391
	M-O	862
Cd-Sb/C	O-H	3379
	M-O	687

d. Band Gap Energy

The band gap energies of the samples were calculated by extrapolating the curve drawn between (h ν) and $(\alpha\ h\nu)^{1/2}$ as shown in the Figures 4.6 and 4.7. The band gap energy obtained by extrapolating the curves was found to be 2.95 and 2.97eV for Cd-Al/AC and Cd-Sb/AC respectively. Li *et al*. (2017) reported that the Zn-Ni-Al calcined at 500^oC has 3.1 eV band which suggest that the catalyst can work well in the visible range.

4.2.2 Operational Parameters

a. Effect of Catalyst Dosage

Dye degradation is also affected by the amount of the photocatalyst used. The dye degradation increases with increasing catalyst concentration, which is characteristic of heterogeneous photocatalysis. The increase in catalyst amount actually increases the number of active sites on the photocatalyst surface thus causing an increase in the number of $^{\bullet}OH$ radicals which can take part in actual discoloration of dye solution. (Shankar *et al*., 2004).

Figure 4.8 shows the degradation efficiency of RB using Cd-Al/AC and Cd-Sb/AC LDHs, with different catalyst dosage after 100 min irradiation at pH 7 condition. The phocatalytic degradation of Rhodamine B increases with increase in the catalyst dosage. This is due to sufficient number of active site on the catalyst surfaces which result in better penetration of visible light. This result is in line with the results obtained by Jahagir *et al*. (2014) in their study of ‘’Photocatalytic degradation of rhodamine B using nanocrystalline Fe_2O_3’’.

From Figure 4.8 most of the photocatalytic studies, investigation of initial rate of photodegradation is found to be proportional to the dose of the catalyst and very vital. The influence of photocatalyst dose on the MR dye degradation was investigated for the dye solutions at an initial concentration of 3 ppm. The visible light photodegradation was done for 100 min with Cd-Al/AC and Cd-Sb/AC catalysts at varying doses in the range of 50–200 mg. The total degradation of MR increased with the increase in Cd-Al/AC and Cd-Sb/AC dose. These results are in line with the results obtained by Singh *et al.* (2014) in their study of ‘’Methyl red degradation under UV illumination and catalytic action of commercial ZnO in which their results showed similar trend’’.

b. Effect of solution pH

The pH value of the aqueous solution is a key parameter for photocatalytic degradation of wastewater and dyes because it affects the adsorption of pollutants that happens at the surface of Photocatalysts (Zielinska *et al.,* 2007).

The effect of pH on photocatalytic degradation of RB by Cd-Sb/AC and Cd-Al/AC is shown in Figure 4.9. It was observed that the effect of photodegration was effective at pH 12. This pH was therefore considered as the optimum pH. It can be due to the increased more production of hydroxyl ions which induce more hydroxyl radical formation. This result is in agreement with the results obtained by Rakhi and Kishore (2017) in their study on ''Investigation of Photocatalytic Degradation of Rhodamine B by Using Nano-Sized TiO_2'' which reported that as the pH increases the oxidizing ability of the holes of semiconductor increases. The hydroxyl radical production made possible the oxidation of hydroxide ions by holes. The more alkaline, the readily hydroxide ions underwent oxidation to generate hydroxyl radicals on the catalyst surface.

From Figure 4.9, the pH solution is important factors that hinders or support a certain reaction. Therefore, in order to study the effect of pH in photodegradation of MR using Cd-Al/AC and Cd-Sb/AC pH values of 5-12 were selected. It was found that at lower pH value of 5 the highest percentage photodegradation of 48.84% for the methyl red was observed. This is due to the electrostatic interactions between a semiconductor surface, substrate, and charge radicals strongly depend on the pH of the solution. This result is in agreement with the results obtained by Thota *et al.,* (2014) in their study of ''visible light induced photocatalytic degradation of methyl red with Co doped TiO_2.'' which reported that as the initial dye concentration increases,

the path length of photons entering the solution decreases, resulting in lower photon adsorption on catalyst particles and, consequently, a lower photodegradation rate.

c. Effect of Dye Concentration

The initial concentration of dye in a given photocatalytic reaction is also another aspect which needs to be taken into account. It is generally found that percentage degradation decreases with increasing amount of dye concentration, while keeping a fixed amount of catalyst (Macedo *et al*., 2007).

Figure 4.10 shows the effect of concentration of dye on photodegradation of RB, in the presences of Cd-Al/AC and Cd-Sb/AC LDHs, respectively. It has been observed that the efficiency of photodegradation of rhodamine B tend to decrease with increasing the concentration of dyes, which results in decrease in the number of active sites and hence decreasing the production of $^{\cdot}OH$ on the surfaces. This result is in agreement with the results obtained by Rakhi and Kishore (2017) in their study investigation of ‘’Photocatalytic Degradation of Rhodamine B by Using Nano-Sized TiO_2’’which reported that it has been observed that the efficiency of photocatalytic degradation of rhodamine B tend to decrease with increase with increasing the concentration of rhodamine B.

By varying the initial concentration from 3 to 12ppm at constant catalysts dosage (200 mg). of Cd-Al/AC and Cd-Sb/AC, its effect on the degradation rate were determined, and the results are shown in Figure 4.10. As seen in the Figure, degradation efficiency of MR increased with decreased in the dyes concentration. These results are in line results with reported by Anitha and Auguestine (2014) in their study of ‘’Photocatalytic Degradation of Alizarin Red S and Bismarck Brown R Using TiO_2Photocatalyst’’ which reported that as the initial dye concentration increases, the path length of photons entering the solution decreases, resulting in lower photon adsorption on catalyst particles and, consequently, a lower photodegradation rate.

Whenever the concentration of dye solution increases, the photons get broken up before they can reach the surface of the catalyst and thus decreases the absorption of photons by the photocatalysts. Due to this reason the photocatalytic degradation rate of the dyes with higher concentration gets reduced (Chakrabarti, 2004).

d. Kinetic Studies

Kinetic studies were employed in order to carefully monitored and intreprete the kinetic of photocalytic process involving two catalysts. The kinetic of the dyes were analysed by pseudo first order and pseudo second order. The results summarized and presented in Table 4.1

1. Pseudo First Order

Pseudo first-order kinetics model (Lagergren 1898) has been most widely used to describe the kinetic process of liquid-solid phase adsorption; i.e., for the adsorption of an adsorbate from an aqueous solution. The linear form of this model is:

$$\log(q_e - q_t) = \log q_e - \frac{K_1}{2.303} t \qquad (13)$$

Where, q_e is the amount of catalysts adsorbed at equilibrium per unit mass (mg/g); q_t is the amount of catalysts adsorbed at time t per unit mass (mg/g); K_1 is the rate constant of pseudo first-order adsorption model ($mg \cdot g^{-1} \cdot min^{-1}$).

K_1 can be evaluated from the graph of log (q_e-q_t) versus t. Such plot will give a straight line for the pseudo first-order adsorption with ($\log q_e$) as intercept and ($-K_1/2.303$) as the slope of the graph.

2. Pseudo second-order kinetics

The adsorption kinetics can also be described by pseudo second-order model. The linear form of this model is given by this equation

$$\frac{t}{q_t} = \frac{1}{K_2 q_e^2} + \frac{1}{q_e} t \quad (14)$$

Where K_2 is the rate constant of pseudo second-order adsorption. If experimental data fit this model, a linear relationship is produced when plotting t/q_t versus t, from which K_2 and q_e can be determined from the slope and intercept from the graph.

From Table 4.1 the calculated correlation coefficients (R^2) is also close to unity for pseudo-second order kinetic than the pseudo-second order kinetic models. Therefore, the photodegradation can be approximated more appropriately by pseudo second order kinetic model (Sumanjit *et al.* (2012). Zhang *et al.*, (2017) reported the correlation coefficients R^2 for the pseudo-second-order model was much larger than that of the pseudo-first-order model

CHAPTER FIVE

5.1 SUMMARY

Degradation of Rhodamine B and Methyl red in aqueous media using synthesized Cd-Al/AC and Cd-Sb/AC LDHs catalysts was investigated. The synthesized catalysts were characterized using Scanning Electron Microscope (SEM), X-ray Diffraction (XRD) and Fourier Transform Infra-red analysis. The absorption peaks in the low frequency region, for M-O is below 862cm^{-1} and 687cm^{-1}in the Cd-Al/AC and Cd-Sb/AC LDHs, respectively. The SEM images showed that the sheet morphology of Cd-Al/AC and Cd-Sb/AC, which indicateds agglomerated grains are not uniform. For the XRD analysis, the average crystallizes size (D values) are 101 and 128 nm for Cd-Al/AC and Cd-Sb/AC respectively. The Cd-Al/C-LDH shown better catalytic activity in all conditions and this is probably due to reduction in band gap energy.

5.2 CONCLUSION

In this research work, the catalysts (Cd-Al/AC and Cd-Sb/AC) were synthesized by copericipitation method. They were characterized using X-ray Diffaraction (XRD), Fourier Infrared Spectrophotometer (FT-IR) and Scanning Electron Microscope (SEM), followed by photo degradation of RB and MR using visible light. The highest degradation efficiencies were achieved at about 100 min, using 200 mg of either Cd-Al/AC or Cd-Sb/AC and at 3ppm concentration of the dye (RB or MR), with percentage removal of 76.22%, 83.8%, 51.36% and 32.36% for RB using Cd-Al/AC, MR using Cd-Al/AC, RB using Cd-Sb/AC and MR using Cd-Sb/AC, respectively. For kinetics studies the data obtained were modeled using pseudo first order and pseudo second order approaches. From the linear regression coefficient values, the data were found to be best fitted to the pseudo second order kinetics. The Cd-Al/C-LDH showed better catalytic activity under all conditions and this is probably due to its low band gap energy.

5.3 RECOMMENDATIONS

The following are the recommendations for further studies:

1. Characterization techniques such as Energy Disperse X-ray (EDX) for percentage composition of the individual elements present in both Cd-Al/AC and Cd-Sb/AC catalysts.
2. Using solar spectrum degradation studies should be carried out.
3. The process should be carried out at the industrial scale, to justify the use of Cd-Al/AC and Cd-Sb/C layered double hydroxide catalysts in the waste water treatment.

REFERRENCE

Adoewi P., Horsfall M. and Spiff A. I. (2012). Adsorption of Methyl Red from Aqueous by Activated Carbon Produced from Cassava (*Manihot esculenta Cranz*) Peel Waste. *Innovations in Sciences and Engineering*, (2) 24-33

Ahmad A., Abdulaziz B. and Muhamad A. (2014). Photodegradation of rhodamine B ove and Applications. *Catalyst Journal*. (3) 189-218.

Al-Rasheed, R.A (2005). Water Treatment by Heterogeneous Photocatalysis. A Review In *Proceedings of the 4th SWCC Acquired Experience Symposium*, Jeddah, Saudi Arabia,

Alrumman S.A., El-kott A.F. and Kehsk M.A. (2016). Water pollution: Source and treatment. *American journal of Environmental Engineering*, 6(3)88-98.

Ameen S., Seo H.K., Akhtar M.S., Shin H.S. (2012). Novel graphene/ polyaniline nanocomposites and its photocatalytic activity toward the degradation of rose Bengal dye. *Chemical Engineering Journal* 210(1): 220-228.

Amor F., A. Diouri, F. Ouanji and M. Kacimi (2018). High efficient photocatalytic activity of Zn-Al-Ti layered double hydroxides nanocomposite. *MATEC Web of Conferences*, (149) 01087

Anitha P and Auguestine A., (2014). Photocacatalytic degradation of Alizarin Red S and Bismarck Brown R using Tio_2 phocatalyst *Journal of Chemistry and Applied Biochemistry* (1) 1-7

Arana, J., Dona-Rodrigves, J.M., Tello-Rendom, E., Carriga Cabo, C., Gonazalus-Diaz, Harrera-Mellian, J.A., Perez-pena J., Colon, G. and Nauio, J.A. (2003). Tio_2 activation by using activated carbon as a support. *Applied Catalysis B, Environmental*, (44) 153.

Arslan I., Balcioglu I.A. and Bahnemann D.W. (2000). Advanced Chemical Oxidation of reactive dyes in simulated dye house effuuents by ferrioxalate-fenton/UV-A and TiO_2 process. *Dyes and Pigments.* 47(3) 207.

Ayawei, N, Angaye S. S. and Wankasi, D (2017). Mg/Fe Layered Double Hydroxide as a Novel Adsorbent for the Removal of Congo red. *International Journal of Applied Science and Technology* (7)83-92

Bibi S, Khan R.L. and Nazir R. (2016). Heavy metals in drinking water of Lakki Marwat District, KPK, Pakistan. *World Applied Sciences Journal*, 34(1)15-19.

Blake D. M., P.-C. Maness, Z. Huang, E. J. Wolfrum, J. Huang, and W. A. Jacoby (1999). Application of the photocatalytic chemistry of titanium dioxide to disinfection and the killing of cancer cells. *Separation and Purification Meterial* (28) 1–50.

Blanco J., Malato S., Fern P., Nez A. and Maldonado M.I. (2009). Review of feasible solar application to water processes. *Renewable and suistanable energy reviews*, (15) 1437-1445

Boehm H.P., Steinle J, Vieweger C. (1977). $Zn_2Cr(OH)_6X.2H_2O$, new layer compounds capable of anion exchange and intracrystalline swelling. *Angewandte Chem*ie *International Journal*, (89)265-276.

Carriazoa D., M. del Arco, E. Garcia-Lopez, G. Marci, C. Martin, L. Palmisano and V. Rives (2011). differenttemperatures,Preparation,characterization and photocatalytic activity in gas–solid regime. *Journal of Molecular Catalysis A*. 342(343) 83–90

Cavani, F., Trifirb, F., and Vaccari, A. (1991). Hydrotalcite Type Anionic Clays: Preparation, Properties and Applications. *Catalysis Today (*11)173-301.

Chakrabart S. and Dutta B.K. (2004). Photocatalytic degradation of model textile dyes in wastewater using ZnO as semiconductor catalyst. *Journal of Hazard Material*. (112) 269-278

Chang Z., Chi M., Fenghua W., Zhigang Y., Jingjing W., Zhongzhu Y., Yongqiu ., Zihao L., Mengying Z., Liuqing S., and Guangming Z (2001). Photocatalytic decomposition of Congo red under visible light irradiation using MgZnCr-TiO_2 layered double hydroxide. *Catalysis Today*, (168) 80-90.

Chawengkijwani C and Y. Hayata, (2008). Development ofTiO_2 powder-coated food packaging film and its ability to inactivate *Escherichia coli* in *vitro* and in actual tests. *International Journal of FoodMicrobiology*, (123) 288–295.

Cho, M.; Chung, H.; Choi, W.; Yoon, J. (2004). Linear correlation between inactivation of *E. coli* and OH radical concentration in TiO2 photocatalytic disinfection. *Water Environmental Resources,* (38) 1069–1077.

Choi S. J., Tae-Hyun K.,Jeong-A L. and Jae-Min O, (2014). Polymer Coated CaAl-Layered Double Hydroxide Nanomaterials for Potential Calcium Supplement *International. Journal of molecular Sciences*, (15*)* 22563-22579.

Colon, G., Hidalgo, M.C., Macias , M. and Navio, J.A. (2003). Influence of residual carbon in the photocatalytic activity of Tio_2/C samples for phenol oxidation. *applied Catalysis B environmental,* (43)163.

Cooper H. L., Maryam I. and Gopal A. (2013).Application of Photocatalysts and LED Light Sources in Drinking Water Treatment. *Catalyst journal*, (3) 726-743.

Davis R.J., Gainer J.L., Neal G.O., Wu I.W. (1994). Photocatalytic decolorization of wastewater dyes. *Water Environmental Resorces* 66(1): 50-53.

Demirbas, A,(2009). Agricultural based activated carbons for the removal of dyes from aqueous solutions: a review. *Journal of Hazardous Materials, (*167) 1-9.

Eggleston, C.M. (2008). Toward new uses for hematite. *Science* (320) 184–185.

El-Gain L., Lakarami M., Sebbar E., and Maghea A. (2009) Removal of Indigo Carmine dye From Water Mg-Al-CO_3 Calcined Layered Double Hydroxide. *Journal of Hazard Material,* (161) 624-632.

El-sayed El-T., A. S. Saleh,R. R. Sheha, A. H. Harb, I and H. H. Someda. (2014). Layered Double Hydroxide/Titanium Semiconducting Materials As a Destructive Photocatalyst for Phenol Removal. *The Egyptian society of Radiation sciences and application* (10) 13-17.

Ferreira C, Domenech S, Lacaze P (2001). Synthesis and characterization of polypyrrole/TiO2 composites on mild steel, *Journal of Applied Electrochemistry* 31(1): 49-56.

Fox ,M.A. and Dulay, M.T., (1993). Heterogeneous photocatalysis. *Chemical Reviews* (93)341-357.

Fujishima A., Rao T. and Tryk D. (2004). Titanium dioxide photocatalysis. *Journal of Photochemical Photobiloogy C,(*1**)**1–21

Fujishima, A., Honda, K., (1972), Electrochemical photolysis of water at a semiconductor electrode. *Nature,* (238) 1-8.

Gasser M.S. and Aly H.F. (2009). Kinetic and adsorption mechanism of Cu(II) and Pb(II) on prepared nanoparticle layered double hydroxide intercalated with EDTA. *Colloids and Surfaces A: Physicochemical and Engineering Aspects,* (336) 167-173.

Goswami D. Y. and D. M. Blake, (1996).Cleaning up with sunshine. *Mechanical Engineering,* (118) 56–59.

Habino T. and Kobayashi M. (2005). Determination of Layered double Hydroxide in water. *Journal of Material Chemistry* (15) 653-656.

Hameed B H. and Akpan U.G. (2009). Parameters affecting the photocatalytic degradation of dyes using TiO_2-based photocatalysts. *Journal harzadous Material* (170) 520-529

Herrmann J. M. (1999). Heterogeneous photocatalysis, fundamentals and applications to the removal of various types of aqueous pollutant. *Catalysis Today*, (55) 115-129.

Hirlekar R. S., Nalawade P., Aware B and Kadam V. J. (2008). Layered double hydroxides: A review. *Journal of Scientific & Industrial Research* (68) 267-272.

Hunger k. (2003). Industrial Dyes Chemistr Properties Applications. *Wiley-VCH Weinheim Cambridge*. 1-643.

Hussein F.H., Attia A.J. and Kadhim S. H. (2007). Photocatalytic Degradation Of Textile Dyeing Waste Water Using Titanium Dioxide and Zinc Oxide. *E-Journal of Chemistry*, 5(2) 219-223

Ibhadon A.O. and Paul F. (2013). Heterogeneous Photocatalysis: Recent Advances. *Nature*, (452) 301-310. https://doi.org/10.1038/nature0659

Inyinbor A.A., Adekola F.A and Olatunji A.G. (2015). Adsorption of Rhodamine B from Aqueous Solution on *Iringia gabonesis* Biomass: Kinetic and Thermodynamics Studies. *South African Journal of Chemistry*, (68) 115-125.

Jahagir A.A., Zulfiqar M.N., Donappa N., Nagabhushana A., and Nagabhushana B.M. (2014) ''Photocatalytic Degradation of Rhodamine B Using nanocrystalline α-Fe_2o_3 *Journal of material of Environmental Sciences*, 5(5) 1426-1433

Jeanette M.C. Robertson, Peter K. J. Robertson, and Linda A. Lawton (2005). A comparison of the effectiveness of TiO_2 photocatalysis and UVA photolysis for the destruction of the the destruction of three pathogenic micro-organism. *Journal of Photochemistry. Photobiology. A: Chemistry.* 175 (1) (2005) 51-57.

Jimin X., Jianjun Z., Min C., Deli J., and Dan W. (2009). Low temperature synthesis of anataserare earth doped titania-silica photocatalyst and its photocatalytic activity under solar-light. *Colloids and Surfaces A Physicochemical Engineering Aspects*, (355) 178–182.

Jung W. C. and Huh Y. D. (1996), Synthesis of Intercatlation compounds between a layered double hydroxides and an anionic dye. *BullKorean Chemical Society*, (17) 547-550.

Kaouther A., Najoua F., and Ezzeddine S. (2017). Photocatalytic decolourization of methylene blue using [Zn-Al] layered double hydroxides synthesized at different molar cationic ratios, *Clay Minerals*, (52) 203–215.

Keller N, Rebmann G, Barraud E, Zahraa O. and Keller V. (2005). Macroscopic carbon nanofibers for use as photocatalyst support. *Catalysis today*, (101)323-329.

Kerc A., Miray B. and Ahmet M.S. (2015). Oxidation of humic acid by photocatalysis. *Ozone Science and Engineering*, 5(6) 497-504.

Khan S. B., Khan S. A. and Asiri A. M. (2016).A fascinating combination of Co, Ni and Al nanomaterial for oxygen evolution reaction, *Applied Surfaces Sciences. (*370) 445–451

Khataee A. and Kasiri M. B. (2010) ''Photocatalytic degradation of organic dyes in the presence of nanostructured titanium dioxide, influence of the chemical structure of dyes'' *Journal of Molecular Catalysis. A Chemistry*. (328) 8–26

Kool H. J., C. F. Keijl, and J. Hrubec, (1985). *Water Chlorination:Chemistry, Environmental Impact and Health Effects*, Lewis,Chelsia, Mich, USA.

Kubin R. (1982). Flourescence quantum yield of some rhodamine dyes. *Journal of Luminescene*, 27(4) 455-462

Kuhn K. P., I. F. Chaberny, K.Massholder, (2003). Disinfectionof surfaces by photocatalytic oxidation with titanium dioxideand UVA light. *Chemosphere*, (53) 71–77.

Kumar A and Pandey G (2017). Photodegradation of Methyl Orange in Aqueos of Visible light active Co:La;Tio_2, Nano Compasite. *Chemical Journal* (8)164.

Lagergren, S. (1898). About the theory of so-called adsorption of soluble substances, *KungligaS venska Vetenskapsaka demine Handlingar*, 24 (4) 1-39.

Lee C., H. Choi, C. Lee, and H. Kim, (2003). Photocatalyticproperties of nano-structured TiO_2 plasma sprayed coating,"*Surface and Coatings Technology*. (173)192–200.

Leroux F, Besse J.P. (2004). Layered Double Hydroxide/polymer nanocomposites. In: Wypych F, editor. Clay surfaces: Fundamentals and applications. *London Elsevier* (1)459-95.

Li Zhang, Qing-Man Liang, Jian-Hui Yan, and Min-Jie Zhou (2017). Synthesis of Composite Oxides Derived from Zn-Ni-Al Layered Double Hydroxides and its Use in Photocatalytic Reduction of CO_2. *International Journal of Advanced Research in Chemical Science (IJARCS), 4(4) 1-10*

Linsebigler, A.L., Lu, G., Yates, J., (1995), Photocatalysis on surfaces: Principles, mecanisms, and selected results. *Chemical Reviews*, (95) 735-758

Macedo L. D., D.A.M.Zaia and G.J. Moore. (2007). Degradation of leather dyeon TiO_2: a study of applied experimental parameters on photoelectrocatalysis, *Journal of Photochemistry and Photobiology A: Chemistry*, (185) 86–93.

Mahmoodi N.N., M. Arami, N.Y. Limaee, N.S. Tabrizi. (2006). Kinetics of heterogeneous photocatalytic degradation of reactive dyes in an immobilized TiO_2 photocatalytic reactor. *Journal of Colloid and Interface Science* (295) 159–164

Malato S., J. Blanco, D. C. Alarc ´on, M. I. Maldonado, P.Fernandez-Ibanez, and W. Gernjak, (2007). Photocatalytic decontaminationand disinfection of water with solar collectors, *Catalysis Today*, (122) 137–149.

Martinez T. Flores-Flores M., E. Luévano-H., Leticia M. Getsemaní M., and Ricardo G. (2018) '' Photocatalytic CO_2 conversion by MgAl layered double hydroxides: Effect of Mg^{2+} precursor and microwave irradiation time. *Journal of Photochemistry and Photobiology* (363) 68-73.

Martos, J., Laire, J. and Harmann J.M. (1989). Dichloromethane photodegradation using titanium catalyst, *Journal of Catalysis* (117);335-347.

Mehra M. and Sharma T.R. (2012). Photocatalytic degradation of two commercial dyes in aqeous phase using photocatalyst TiO_2. *Advances in Applied Research*, 3(2) 849-853.

Meng-Qiang Z., Qiang Z., Jia-Qi H., Jing-Qi. N and Fei W. (2010). Layered double hydroxides as catalysts for the efficient growth of high quality single-walled carbon nanotubes in a fluidized bed reactor. *Material Sciences*, (4 8) 3 2 6 0 –3 2 7 0

Merina P. D., Manas B. And Maggidi R. (2016). Biological Decolorization Of Carcinogenic Azo Dye: An Ecofriendly Approach. *International Journal of Pharmacetical and Biology Sciences*. (3) 1164-1170.

Milica S. H., Tatjana J. V. and Radmila P M. (2010). A study of thermally activated Mg–Fe layered double hydroxides as potential environmental catalysts, *Journal of Serbian Chemical Society. 75* (9) 1251–1257.

Mills, A., LeHunte, S., (1997). An overview of semiconductor photocatalysis. *Journal of Photochemistry and Photobiology*. A (108)1-35.

Minero, C., Cattazo, F. and Pelizetti E. (1992). Role of adsorption in photocatalysed reactions of organic molecules in aqueous TiO_2 suspension, *Langmuir* 8(**2**)481-486.

Molina S. and Rodrigues R. F. (2004). Physicochemical and engineering aspect, *Colloids and Surfacea A*, (241) 15-25.

Ng C.M., Chen P.C., Manickam S (2012). Hydrothermal crystallization of titania on silver nucleation sites for the synthesis of visible light nano-photocatalysts-Enhanced photoactivity using Rhodamine 6G,. *Applied Catalysis A*: *General* (433) 75-80.

Nguyen T. T., Han P. N., Nguyen Q. V. and Hong D. K. (2017). Advanced oxidation of rhodamine B with hydrogen peroxide over Zn-Cr layered double hydroxide catalysts. *Advanced Materials and Devices*, (2) 317-325

Pang, Y. L & Abdullah, A. Z.(2013). Current Status of Textile Industry Wastewater Management and Research Progress in Malaysia, A Review. Clean (Weinh) (41) 751–764.

Papic, S., Koprivanac, N., Bozic, A. and Metes, M. (2004). Removal of Some Reactive Dyes from Synthetic Wastewater by Combined Al(III) Coagulation/Carbon Adsorption Process, *Dyes and Pigments* (62) 291-298. https://doi.org/10.1016/S0143-7208(03)00148-7

Parida, K. M., Baliarsingh, N., SairamPatra, B., and Das, J. (2006). Copper Phthalocyanine Immobilized Zn/Al LDH as Photocatalyst under Solar Radiation for Decolorization of Methylene Blue, *Journal of Molecular Catalysis A: Chemical (*267): 202-208.

Parmon V.; Emeline A. and Serpone N. (2002). Spectral selectivity of photocatalysed reaction in liquid-solid photosystem. *International Journal Photoenergy* (4) 91.

Pignatton J. and Sun J. (1995). Mechanism of slow sorption of organic chemicals to natural particles. *critical reviews in environmental sciences and technology*, 30(1)1-11.

Popoola V.A (2015). The Chemistry of Colours in Dyes and Pigment, Wits Publishind Ltd.

Press,

Rakhi G and Kishore D., (2015). Investigation Of Photocatalytic Degradation of Rhodamine B by using Nana Sized Tio_2, *International Journal of Scientific Research and Management (IJSR),* 5 (9) 6006-6013.

Rauf M. A., S.B. Bukallah, A. Hammadi, A. Soliman, F. Hammadi. (2007). The effect of operational parameters on the photoinduced decoloration of dyes using a hybrid catalyst V_2O_5/TiO_2. *Chemical Engineering Journal*, (129) 167–172

Ren N., Charlton J. and Alder P.N. (2007). The flare gene, which encodes the AIPI protein Dros Phila, function to regulate F-action disassembly in popular epidermis cells, *Genetics* 176 (4) 2223-2234

Reza K.M., Kurny A.S.W., Gulshan F. (2017). Parameters affecting the photocatalytic degradation of dyes using TiO_2 a review. *Applied Water Science*, 7(4): 1569-1578.

Saravanan R., Francisco G. and Stephen A. (2017). Basic Principles, Mechanism, and Challenges of Photocatalysis. *Department of Chemical Engineering and Biotechnology, University of Chile*, (10) 3-319.

Shahid A. K., Sher B. K., and Abdullahi M. A. (2016).Layered double hydroxide of Cd-Al/C for the Mineralization and De-coloration of Dyes in Solar and Visible Light Exposure. *Scientific report*, (10) 1038-1052.

Shankar M.V.; KK Cheralathan; B Arabindoo; M Palanichamy; V Murugesan(2004). Enhanced photocatalytic activity for the destruction of monocrotophos pesticide by TiO_2. *Journal Molecular Catalyst A Chemistry,* **(**223) 195-200.

Shannon, M.A., Bohn, P.W., Elimelech, M., Georgiadis, J.G., Marinas, B.J. and Mayes, A.M. (2008). Science and Technology for Water Purification in the Coming Decades. *Nature* , 301-310. https://doi.org/10.1038/nature06599

Sheng-JieX., Feng-Xian L., Zhe-Ming N., Ji-Long X., Ping-Ping Q. (2013). Layered double hydroxides as efficient photocatalysts for visible-light degradation of Rhodamine B. *Journal of Colloid and Interface Science*, (405) 195-200

Siew T. O., Wai S. C.and Yung T. H. (2012). Photodegradation of Commercial Dye, Methylene Blue Using Immobilized TiO_2. *International Conference on Chemical, Biological and Environmental Engineering* (43)23-30

Singh N.k., Sandip S. and Anjali P.(2014). Methyl Red Degradation Under UV illumination and catalytic action of commercial ZnO. *Journal of Desllination and Water Treatment* (56) 1066-1076

Skorb E. V, L. I. Antonouskaya, N. A. Belyasova, D. G.Shchukin, H. M¨ohwald, and D. V. Sviridov, (2008), Antibacterialactivity of thin-film photocatalysts based on metal-modified TiO_2 and TiO_2:In_2O_3 nanocomposite. *Applied Catalysis B*, (84) 94–99.

Soke K T, Tjoon T T, Abbas F.M. Alkarkhi, Zhimin L. (2012). Sonocatalytic Degradation of Rhodamine B in Aqueous Solution in the Presence of Tio_2 Coated Activated Carbon. International Journal of Environmental Sciences and Development, (1) 110-115

Somorjai G. (1989). Photocatalysis - Fundamentals and Applications, Chapt.9.N. Serpone and E. Pelizzetti (eds.), Wiley-Interscience, New York-London, chapters 1,2,5

Sriparna C., Avesh K. T. and Pushan A. (2014). Efficient Photocatalytic Degradation of Rhodamine B Dye by Aligned Arrays of Self-Assembled Hydrogen Titanate Nanotubes, *Journal of Nanomaterial* (10) 1155.

Sumanjit K. Seema R. and Rakesh K.M. (2006). Adsorption Kinetics For Removal of the Hazardous Dye Congo Red by Biowaste material as adsorbents. *Journal of Chemistry* (10) 1155-1162.

Sung-Ho H., Yang-Su H. and Choy J H., (2001). Intercalation of Functional organic molecules with pharmaceutical, cosmeceutical and nutraceutical functions into Layered double hydroxides and Zinc basic salts, *Bull Korean Chemical Society, (*22**)**1019-1022

Tanaka T., S. Nishimoto, Y. Kameshima, J. Matsukawa, Y. Fujita, Y. Takaguchi, M. Matsuda, M. Miyake, (2010). A novel nanocomposite material prepared by intercalating photoresponsivedendrimers into a layered double hydroxide. *Journal Solid State Chemistry***,** (183) 479-483.

Taylor R.M. (1984). The rapid formation of crystalline double hydroxy salts and other compounds by controlled hydrolysis. *Clay Mineral*, (19)591-603.

Thota S., Siva R. T and Sreedhar B. (2014). Visible light photocatalytic Degradation of Methyl Red with Codoped Titanium. *Journal of catalysts*, (1155) 9624

Tompkins D. T., W. A. Zeitner, B. J. Lawnicki, and M. A. Anderson (2005). Evaluation of photocatalysis for gas-phase aircleanin—part 1: process, technical, and sizing considerations. *Ashrae Transactions*, (111) 60–84.

Turabik M. (2008). Adsorption of basic dyes rom single and binary component systems onto bentonite: Simultaneous analysis of Basic red 46 and basic yellow 28 by first order derivatives spectrophotometric analysis method, *Journal of hazardous material, (*158)52-64.

Turchi C. S., Edmunson L., and Ollis D.P. (1989). Application of heterogeneous photocatalysis for the destruction of organic contaminants from a paper mill alkali extraction process, in *Proceedings of the TAPPI 5th International Symposium on Wood and Pulping Chemistry*, Raleigh, NC, USA.

Ulibarri M. A., Barriga, C., Pavlovic, I., Hermosin, M. C. and Cornejo, J., (2002) ‘’Hydrotalcites as sorbent for 2,4,6-trinitrophenol: Influence of the layer composition and interlayer anion’’ *Journal of Materials Chemistry*, (12)1027-1034.

Wai M., Mingfei S., Jingbin H., David G. E.and Xue D. (2011). The synthesis of hierarchical Zn–Ti layered double hydroxide for efficient visible-light photocatalysis. *Chemical engineering journal*, (162) 1385-8947.

Wang J.A, Morales A, Bokhimi X, Novaro O, Lopez T, Gomez R. (1999). Aluminum local environment and defects in the crystalline structure of sol-gel alumina Catalyst. *Journal of Physical Chemistry B.* (103)299-303.

Wang Q, Tang SV, Lester E, O’hare D. (2013). Synthesis of ultrafine layered double hydroxide (LDH) nanoplates using a continuousflow hydrothermal reactor. *Nanoscale*, (5)114-7.

Wei M., Lei T., Yufei Z., Shan H. and Xue Duan (2012). Immobilized Cu–Cr layered double hydroxide films with visible-light responsive photocatalysis for organic pollutants. *Chemical Engineering Journal*, (184) 261-267.

Wong F., and Buchheit R. G., (2004). Utilizing the structural memory effect of layered double hydroxides for sensing water uptake in organic coatings. *Progress in Organic Coatings,*(51) 91–102.

Yao K. S., Wang D. Y., Ho W. Y., Yan J. J., and Tzeng K. C., (2007). Photocatalytic bactericidal effect of TiO2 thin film on plant pathogens. *Surface and Coatings Technology*, (201) 6886–6888.

Yasuo I., Shogo K., Naveed A., and Gabriela C.(2015). Photocatalytic Conversion of Carbon Dioxide Using Zn–Cu–Ga Layered Double Hydroxides Assembled with Cu Phthalocyanine, Cu in Contact with Gaseous Reactant is Needed for Methanol Generation’’ *IFP Energies nouvelles* (5) 842-852.

Ye J., Morimoto K., Tamura K. and Yamada H. (2012). Photocatalytic Degradation of Anionic Dye by Zn-Substitued Layered Double Hydroxide in aqueous solution. *Transtions of the Material Research Society*, 37(1) 19-22.

Yong R.L.,Nagaraj B. and Kanchan M. (2017). Trimetallic FeAgPt alloy as a nanocatalyst for the reduction of 4-nitroaniline and decolorization of rhodamine B: A comparative Study. *Journal of Alloys and Compounds* (701) 456-464.

Yudong H., Ommeaymen S. Feng Z. Ali R. and Erfan K. (2014). Precursor and Reaction Time Effect in Evaluation of Photocatalytic Properties of TiO_2 Nanoparticles Synthesized Via Low Temperature, *International Journal of Electrochemical Sciences* (9) 3068-3077.

Zhang G., Shan C., Huifang T. and He Z. (2016).Rapid degradation of dyes in water by magnetic Fe0/Fe3O4/graphene composites. *Journal of Environmental Sciences*, (44) 148-157.

Zhang X, Zhou M. and Lei L (2006). TiO_2 photocatalyst deposition by MOCVD on activated carbon. *Chemistry Material* (44) 325-233.

Zhang X.H., Axton J.M., Drinjakovic J., Lorenz L White-Cooper H. and Renault A.D. (2004). Spatial and Temporary Control of Mitotic Cyclins by the Gnu regulator by the embryonic mitosis in Drosophila, *Journal of Cell Sciences,* (16) 3571-3578.

Zhang Y., Pan H., Fengzhu L., Wangshu T., Hao X., Zilin M., Xinke W. and Paul K. (2017). Preparation of layered double hydroxides using boron mud and red mud industrial wastes and adsorption mechanism to phosphate. *Water and Environment Journal*, (31) 145–157

Zhao Y, Li F, Zhang R, Evans DG, Duan X. (2002). Preparation of layered double-hydroxide nanomaterials with a uniform crystallite size using a new method involving separate nucleation and aging steps. *Chemistry Material*, (14)4286-91.

Zhao, H., Xu, S., Zhong, J. and Bao, X. (2004). Kinetic Study on the Photocatalytic Degradation of Pyridine in TiO_2. *Catalysis Today*, (93) 857-861.

Zhe-Ming N., Sheng-Jie X., Feng-Xian L., Ji-Long X., and Ping-Ping Q. (2017). Layered double hydroxides as efficient photocatalysts for visible-light degradation of Rhodamine B, *Journal of Colloid and Interface Science* (405) 195–200.

Zhu J., Deng Z., Chen F., Zhang J. and Chen H. (2006). Hydrothermal doping method for preparation of Cr^{3+}-TiO_2 photocatalysts with concentration gradient distribution of Cr^{3+} *Applied Catalysis B Environmental* 62(3) 329-335.

Zielińska B., Grzechulska J., Kaleńczuk R.J. and Morawski A.W. (2003). The pH influence on photocatalytic decomposition of dyes overA11 and P25 titanium dioxide. *Applied Catalysis B*: *Environmental* 45(4), 293–300.

APPENDICES

Appendix 1

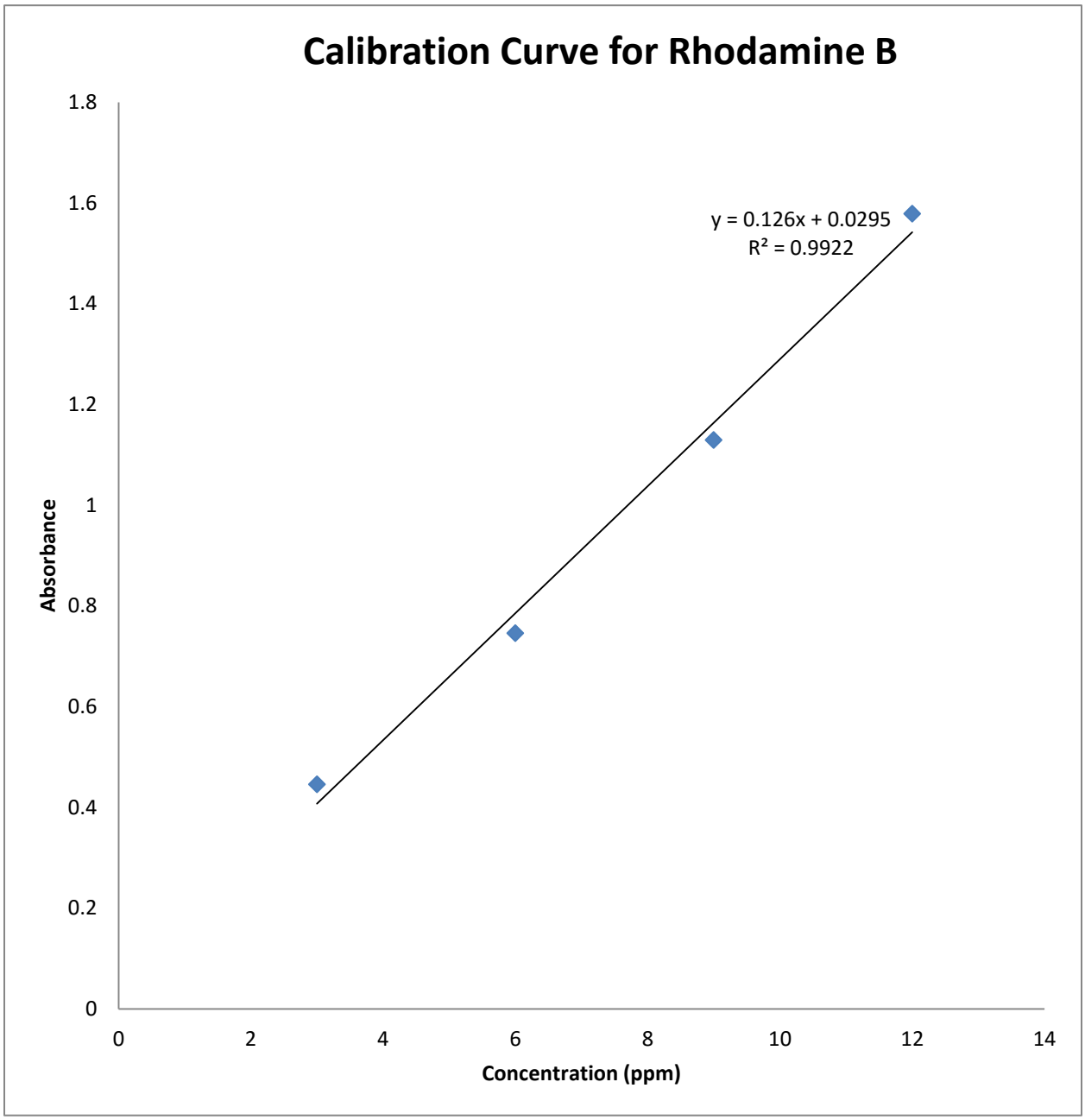

Calibration Curve for Rhodamine B

Appendix 2

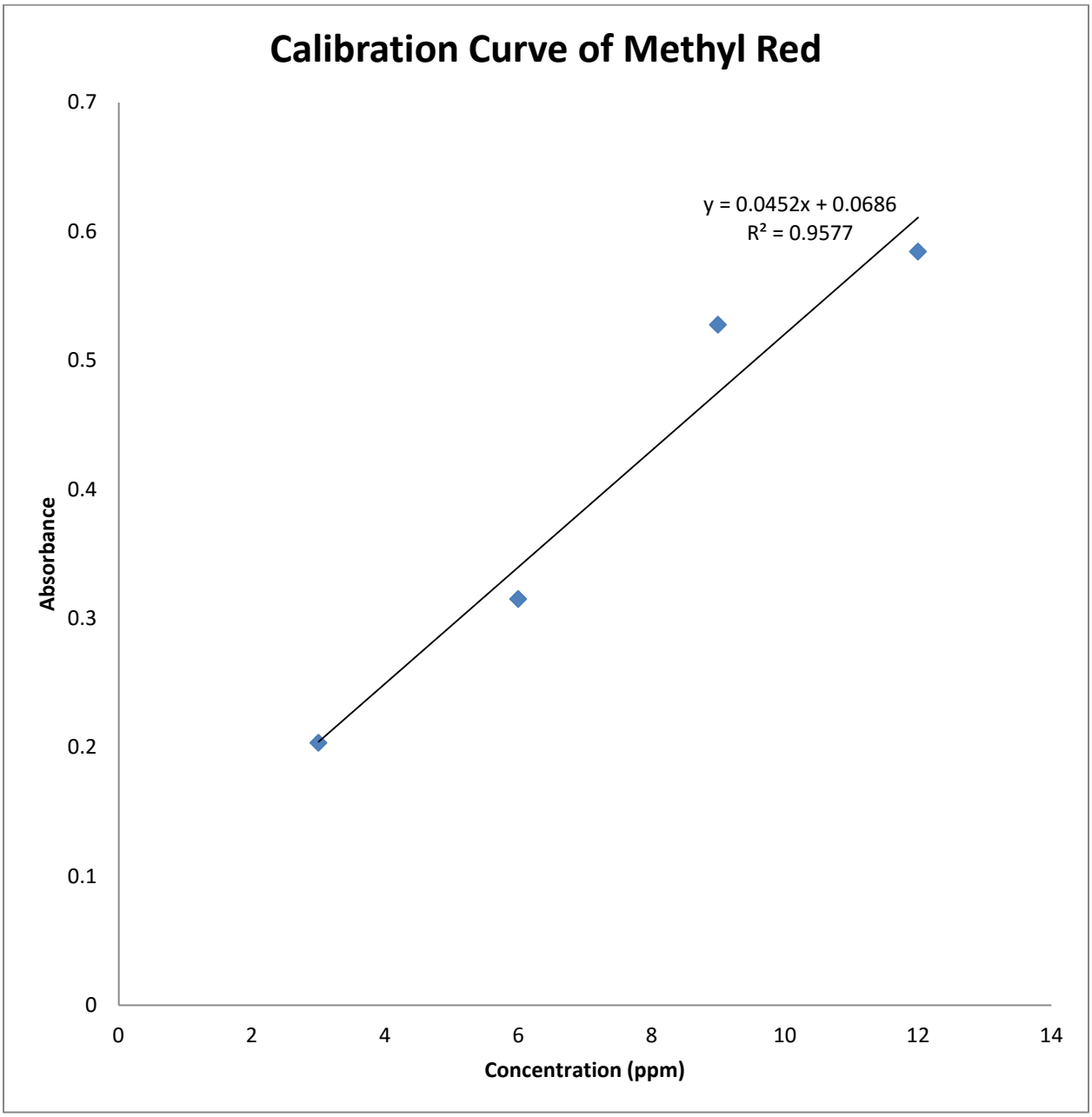

Carlibration curve of methyl red